Published by
NIGERIAN SOCIETY OF PHYSICAL SCIENCES
Available online @ https://journal.nsps.org.ng/index.php/jnsps

J. Nig. Soc. Phys. Sci. 9 (2027) 3812

Journal of the Nigerian Society of Physical Sciences

Dynamics and stability of a fractional-order renewable resource model with generalized Mittag-Leffler kernel and fractal dimension

Kottakkaran Sooppy Nisar[a,b], Anum Zehra[c,d], Evren Hincal[d,e], Mustafa Bayram[f], Muhammad Farman[d,g,h,*]

[a]*Department of Mathematics, College of Science and Humanities in Al Kharj, Prince Sattam bin Abdulaziz University, Al Kharj, 16277, Saudi Arabia*
[b]*Hourani Center for Applied Scientific Research, Al-Ahliyya Amman University, Amman, Jordan*
[c]*Department of Mathematics, The Women University Multan, Multan, Pakistan*
[d]*Department of Mathematics, Mathematics Research Center, Near East University, Mersin-10, Turkey*
[e]*Research Center of Applied Mathematics, Khazar University, Baku, Azerbaijan*
[f]*Department of Computer Engineering, Biruni University, 34010 Topkapi, Istanbul, Turkey*
[g]*Faculty of Medicine, Department of Biostatistics and Medical Informatics, Karadeniz Technical University, Trabzon, Turkey*
[h]*International Center for Interdisciplinary Research in Sciences, The University of Lahore, Lahore, Pakistan*

Abstract

Fractional-order derivatives have a wide range of applications in real-world problems. In this work, we focus on a renewable resource in biomass management with population effects using a generalized Mittag-Leffler kernel. We modify the system into a time-fractional-order biomass model with population impacts on resource biomass while accounting for the suffocation effect, and analyze its dynamics under the Atangana–Baleanu Caputo (ABC) fractional operator. We establish positivity, boundedness, existence, and uniqueness of the fractional-order model using fixed-point theory. We confirm global stability by means of the fractional derivative of a Lyapunov function and compute Ulam–Hyers stability using the spectral radius of the associated matrix. The proposed model has a unique solution according to the Banach contraction principle. The numerical scheme for the fractal-fractional Atangana–Baleanu Riemann–Liouville (ABR) extension of the ABC model is constructed using a two-step Lagrange polynomial in the generalized form of the Mittag-Leffler kernel. Simulations are carried out at various parameter values, fractional orders, and fractal dimensions. The numerical results reveal that the dynamics vary significantly with fractional order, leading to either convergence to a steady state or oscillatory behavior. The study offers a framework for capturing population-resource interactions and demonstrates how fractional order can inform control of biomass consumption under population pressure. These insights are useful for planning and decision-making regarding the social impact of biomass.

DOI: 10.46481/jnsps.2027.3812

Keywords: Model of biomass, Stability, Modeling, Fixed-point theory, Fractional derivative

Article History:
Received: 09 August 2026
Received in revised form: 19 September 2026
Accepted for publication: 20 September 2026
Available online: 10 November 2026

© 2027 The Author(s). Published by the Nigerian Society of Physical Sciences under the terms of the Creative Commons Attribution 4.0 International license. Further distribution of this work must maintain attribution to the author(s) and the published article's title, journal citation, and DOI.

Communicated by: B. J. Falaye

1. Introduction

Renewable resources are a significant source of food and materials for the development and survival of biological populations. Continuous and unregulated exploitation of these re-

*Corresponding Author Tel. No.: +90-539-131-8241.
Email address: farmanlink@gmail.com (Muhammad Farman)

sources might lead to resource extinction, putting the survival of resource-dependent species in jeopardy. Over the course of a year, traditional cooking and heating are used globally. Traditional bioenergetics are not sustainable, according to the International Energy Agency (IEA), and will be phased out by 2030 under its Net Zero by 2050 scenario. Commercial fishing dynamic models have been widely investigated, taking into consideration economic and ecological issues [1]. Non-explosive fishing capital investment and non-extinctive fisheries resources were explored by Wang *et al.* [2], who provided a basic economic model. They discussed the bionomical equilibrium and the ideal harvesting approach while looking at the stability analysis.

In the positive quadrant, there is no limit cycle. Brown [3] suggested a scenario in which the predator is selectively collected and the prey has no financial value. In order to successfully manage these resources and prevent catastrophic explosions in our global economy, mathematical bio-economics may play a significant role. It may consider how this demand might influence the resource as well as difficulties with revenue, cost, etc. [4]. Samanta [5] discussed harvest competition and bionomic equilibrium in society. According to Ref. [6], the stability and Hopf-bifurcation of a two-species, multi-delayed, competitive system impacted by hazardous substances were proposed. The Susceptible-Infected-Recovered model has been studied in Ref. [7]. Along with the identification of equilibrium points and the conditions necessary for their viability, the stability of the system is studied [8].

Projects using fish, barbecued chickens, and ducks have been found to be suitable for the three-species harvesting technique. Recent studies demonstrate that complex mathematical models effectively describe nonlinear processes in physical and biological systems.

A new method for the fractional calculus fractal fractional derivative is currently being developed by Atangana [9]. The concept underlying this topic is often highly suitable for resolving some challenging problems. The notion of the fractional derivative based on the power law is introduced by Riemann Liouville. The novel fractional derivative that uses the exponential-decay kernel was proposed by Caputo and Fabrizio [10]. The non-singular kernel fractional derivative that incorporates trigonometric and exponential functions was introduced by Caputo and Fabrizio [10]. Recent studies have applied fractional-order derivatives to neural network models: Xu *et al.* [11, 12] analyzed the dynamical properties and bifurcation behavior of fractional-order delayed bidirectional associative memory (BAM) neural networks. Further studies according to Ref. [13] examined delay-induced periodic oscillations in fractional-order neural networks with mixed delays, and Xu *et al.*

[14] investigated the bifurcation dynamics and control mechanism of a fractional-order delayed Brusselator chemical reaction model. One important dynamical feature in nonlinear delayed differential models is Hopf bifurcation triggered by delay. In chemistry, the transformation relationship of the concentration of various chemical compounds can be readily characterized by Hopf bifurcation triggered by delay. Thus, we contend that investigating the Hopf bifurcation caused by delay in different chemical reaction models is crucial [15, 16]. Delay-driven Hopf bifurcation has also been studied in epidemiological settings, for example in a networked malaria model [17]. Fractional calculus has grown in importance due to its demonstrated applications in system biology and other scientific domains [18]. One advantage of fractional and integral derivatives is that they are not local (or point) quantities.

This non-local character has been exploited, for example, in epidemic models on random networks with multiple routes of transmission [19]. We found that in order to understand the complexity of infectious diseases, epidemiologists often use mathematical models. The disease modeling method with controls is studied using the stability theory of differential equations [20]. Bankole *et al.* [21] investigated the optimal control of fractional-order stochastic systems under uncertainty, incorporating Poisson and V-jump perturbations. Olaniyi *et al.* [22] analyzed the asymptotic stability of a fractional-order Ebola epidemic model using the Caputo fractional derivative, highlighting the role of fractional calculus in capturing the dynamics of biological systems. The most widely used operators, such as Atangana-Baleanu and Caputo-Fabrizio, use a local derivative with a distinct function.

However, complex fractal behavior can be seen in real-world phenomena such as biomedicine and volatility. In this instance, operators involving non-local differentiation in the kernel are required [23] provide fractional fractal operators. The epidemiological patterns that fractional operators support include dengue fever, TB, measles, Ebola, and other diseases. However, the ongoing debate on the foundations and applicability of fractal-fractional operators has been discussed by Atangana [24], who argues that their efficacy depends on the choice of kernel and on the specific application.

Although various works have been done on the subject of fractional order population-resource models, there are still several areas that demand additional investigation. These models often employ either the Caputo or Caputo-Fabrizio operators; relatively few studies include both the Atangana–Baleanu Caputo (ABC) operator, the generalized Mittag-Leffler kernel, and the suffocation effect in biomass population systems. This work attempts to address these constraints by providing a time-fractional biomass model that incorporates the influence of population on biomass via the ABC operator. The global and Ulam-Hyers stability are examined using fractional Lyapunov and spectral radius approaches and applied to the fractal-fractional Atangana–Baleanu Riemann–Liouville (ABR) operator, resulting in solid demonstrations of existence and uniqueness. The research emphasizes the importance of using a memory-dependent technique to control biomass under population pressure while taking fractional order and fractal dimension into account.

The remaining sections of this article are structured as follows. Section 2 provides some preliminary information on the ABC fractional derivative and fixed point theory techniques. Section 3 formulates the fractional biomass model and uses fixed point techniques, along with Ulam-Hyers stability for the spectral radius of the corresponding matrix, to establish the ex-

istence and uniqueness, positivity, and boundedness of solutions to the proposed model. Section 4 studies the equilibrium points of the model, providing conditions for global asymptotic stability using the fractional Lyapunov function technique and generalizing existence and uniqueness results for the fractal-fractional ABR case. Section 5 describes how the numerical technique was developed utilizing the ABC Fractal Operator and Lagrangian Piecewise Interpolation. Section 6 discusses the numerical simulation results. Section 7 concludes the paper and discusses future work.

2. Basic concepts

In this section, we discuss some important definitions which are useful for solving the problem.

Definition 2.1. [25] If $\psi \in H_1(0,T)$ and $\varphi \in (0,1]$, then the ABC derivative is defined by

$$ {}^{ABC}D_t^{\varphi}\psi(t) = \frac{\kappa(\varphi)}{1-\varphi}\int_0^t \frac{d}{dy}\psi(y)E_{\varphi}\left[\frac{-\varphi}{1-\varphi}(t-y)^{\varphi}\right]dy. \quad (1)$$

By replacing $E_{\varphi}\left[\frac{-\varphi}{1-\varphi}(t-y)^{\varphi}\right]$ with $E_1 = \exp\left[\left(\frac{-\varphi}{1-\varphi}\right)(t-y)\right]$, it has been observed that

$$ {}^{ABC}D_t^{\varphi}[\text{Constant}] = 0. \quad (2)$$

Here, $K(\varphi)$ is the normalization function which is given as $K(0) = K(1) = 1$. E_{φ} denotes the Mittag-Leffler kernel.

Definition 2.2. [25] Given $\psi \in L(0,T)$, the equivalent integral in the ABC sense is as follows:

$$ {}^{ABC}I_t^{\varphi}\psi(t) = \frac{1-\varphi}{K(\varphi)}\psi(t) + \frac{\varphi}{K(\varphi)\Gamma(\varphi)}\int_0^t (t-y)^{\varphi-1}\psi(y)dy. \quad (3)$$

Lemma 2.1. [26] The answer to the provided problem for $1 > \varphi > 0$,

$$ {}^{ABC}D_t^{\varphi}\psi(t) = \theta(t), \quad t \in [0,T], \quad \psi(0) = \psi_0, \quad (4)$$

is given by

$$ \psi(t) = \psi_0 + \frac{(1-\varphi)}{K(\varphi)}\theta(t) + \frac{\varphi}{\Gamma(\varphi)K(\varphi)}\int_0^t (t-y)^{\varphi-1}\theta(y)dy. \quad (5)$$

Lemma 2.2. Assume that B is a convex subset of Z and that F and G are two operators.

1. $G(Z) + F(Z) \in B$ for every $Z \in B$;
2. F denotes a contraction;
3. G is compact and continuous.

There is at least one solution for the equation operator $G(Z) + F(Z) = Z$, in which $Z = (Q, R)$ [27].

3. Mathematical model with fractional operator

The investigation indicates that when harvesting a renewable resource that a population consumes for its own growth and development, the impact of crowding has not been taken into account. As a result, the author of this work presents a mathematical model for a biological population that is heavily reliant on renewable resources. In order to investigate the dynamics of biomass resources and population usage, the model presented in Ref. [28] was modified with a fractional operator.

$$ \begin{cases} \frac{dQ}{dt} = rQ(1-\frac{Q}{\mathcal{K}}) - \alpha_1\mathcal{R}Q - \alpha_2\mathcal{R}Q^2 - q\mathcal{E}Q, \\ \frac{d\mathcal{R}}{dt} = s\mathcal{R}(1-\frac{\mathcal{R}}{\mathcal{L}}) + \beta_1\mathcal{R}Q - \beta_2\mathcal{R}Q^2, \end{cases} \quad (6)$$

with initial conditions $Q(0) > 0$ and $\mathcal{R}(0) > 0$. The population density, denoted by $Q(t)$ for the population and $\mathcal{R}(t)$ for the resource biomass density, will determine the intrinsic growth rate and carrying capacity of the biomass. The following nonlinear differential equation represents the proposed model with the ABC derivative.

$$ \begin{cases} {}^{ABC}D_t^{\varphi}Q = rQ(1-\frac{Q}{\mathcal{K}}) - \alpha_1\mathcal{R}Q - \alpha_2\mathcal{R}Q^2 - q\mathcal{E}Q, \\ {}^{ABC}D_t^{\varphi}\mathcal{R} = s\mathcal{R}(1-\frac{\mathcal{R}}{\mathcal{L}}) + \beta_1\mathcal{R}Q - \beta_2\mathcal{R}Q^2, \end{cases} \quad (7)$$

$$ \begin{cases} {}^{ABC}D_t^{\varphi}Q = f(t,\mathcal{Z}), \\ {}^{ABC}D_t^{\varphi}\mathcal{R} = g(t,\mathcal{Z}), \end{cases} \quad (8)$$

where $\mathcal{Z} = (Q,\mathcal{R})$. Using the Lemma with initial conditions and applying the fractional ${}^{AB}I_t^{\varphi}$ of order φ on both sides, we obtain

$$ \begin{aligned} Q &= Q_0 + \frac{1-\varphi}{\mathcal{K}(\varphi)}f(t,\mathcal{Z}) + \frac{\varphi}{\Gamma(\varphi)\mathcal{K}(\varphi)}\int_0^t (t-y)^{\varphi-1}f(y,\mathcal{Z}(y))dy, \\ \mathcal{R} &= \mathcal{R}_0 + \frac{1-\varphi}{\mathcal{K}(\varphi)}g(t,\mathcal{Z}) + \frac{\varphi}{\Gamma(\varphi)\mathcal{K}(\varphi)}\int_0^t (t-y)^{\varphi-1}g(y,\mathcal{Z}(y))dy, \end{aligned} \quad (9)$$

where $\mathcal{Z} = (Q,\mathcal{R})$ and $\mathcal{Z}(y) = (Q(y),\mathcal{R}(y))$. We have used some conditions to derive uniqueness and existence for the nonlinear functions $f, g : [0,\mathbb{T}] \times \mathcal{K} \times \mathcal{K} \to \mathcal{K}$.

- For any $Q, \overline{Q}, \mathcal{R}, \overline{\mathcal{R}} \in \mathcal{R}$, there are constants $\mathcal{L}_f, \mathcal{L}_g > 0$ such that

$$ |f(t,\mathcal{Z}) - f(\bar{t},\overline{\mathcal{Z}})| \le \mathcal{L}_f\left[|Q-\overline{Q}| + |\mathcal{R}-\overline{\mathcal{R}}|\right], \quad (10)$$

$$ |g(t,\mathcal{Z}) - g(\bar{t},\overline{\mathcal{Z}})| \le \mathcal{L}_g\left[|Q-\overline{Q}| + |\mathcal{R}-\overline{\mathcal{R}}|\right], \quad (11)$$

where $\mathcal{Z} = (Q,\mathcal{R})$ and $\overline{\mathcal{Z}} = (\overline{Q},\overline{\mathcal{R}})$.

- There exist constants $C_f, C_g, \mathcal{B}_f, \mathcal{B}_g > 0$ and $\mathcal{M}_f, \mathcal{M}_g > 0$ such that

$$ |f(t,\mathcal{Z})| \le C_f|Q| + \mathcal{B}_f|Q| + \mathcal{M}_f, \quad (12)$$

$$ |g(t,\mathcal{Z}(t))| \le C_g|\mathcal{R}| + \mathcal{B}_g|\mathcal{R}| + \mathcal{M}_g. \quad (13)$$

Theorem 3.1. Under the second assumption and the continuity of f and g, the system has at least one solution if $\left(\frac{1-\varphi}{\mathcal{K}(\varphi)}\right)\mathcal{L}<1$, where $\mathcal{L} = \max\{\mathcal{L}_f, \mathcal{L}_g\}$.

Proof. Krasnoselskii's fixed point theorem can be used to verify existence results. The operators $\mathcal{F} = (\mathcal{F}_1, \mathcal{F}_2)$ and $\mathcal{G} = (\mathcal{G}_1, \mathcal{G}_2)$ are defined as follows.

$$\begin{cases} \mathcal{F}_1\mathcal{Z} = \mathcal{Q}_0 + \frac{1-\varphi}{\mathcal{K}(\varphi)} f(t, \mathcal{Z}(t)), \\ \mathcal{G}_1\mathcal{Z} = \frac{\varphi}{\Gamma(\varphi)\mathcal{K}(\varphi)} \int_0^t (t-y)^{\varphi-1} f(y, \mathcal{Z}(y))dy, \\ \mathcal{F}_2\mathcal{Z} = \mathcal{R}_0 + \frac{1-\varphi}{\mathcal{K}(\varphi)} g(t, \mathcal{Z}(t)), \\ \mathcal{G}_2\mathcal{Z} = \frac{\varphi}{\Gamma(\varphi)\mathcal{K}(\varphi)} \int_0^t (t-y)^{\varphi-1} g(y, \mathcal{Z}(y))dy. \end{cases} \tag{14}$$

Consequently, $\mathcal{G}$ is a continuous operator while $\mathcal{F}$ is a contraction. For every $\mathcal{Z}, (\overline{\mathcal{Q}}, \overline{\mathcal{R}}) \in \mathcal{B}$, we have

$$|\mathcal{F}_1(t, \mathcal{Z}(t)) - \mathcal{F}_1(\bar{t}, \overline{\mathcal{Z}(t)})| \leq \frac{1-\varphi}{\mathcal{K}(\varphi)} \mathcal{L}_f [|\mathcal{Q} - \overline{\mathcal{Q}}| + |\mathcal{R} - \overline{\mathcal{R}}|], \tag{15}$$

which suggests that

$$\|\mathcal{F}_1(t, \mathcal{Z}(t)) - \mathcal{F}_1(\bar{t}, \overline{\mathcal{Z}(t)})\| \leq \frac{1-\varphi}{\mathcal{K}(\varphi)} \mathcal{L}_f [\|\mathcal{Q} - \overline{\mathcal{Q}}\| + \|\mathcal{R} - \overline{\mathcal{R}}\|], \tag{16}$$

$$\|\mathcal{F}_2(t, \mathcal{Z}(t)) - \mathcal{F}_2(\bar{t}, \overline{\mathcal{Z}(t)})\| \leq \frac{1-\varphi}{\mathcal{K}(\varphi)} \mathcal{L}_g [\|\mathcal{Q} - \overline{\mathcal{Q}}\| + \|\mathcal{R} - \overline{\mathcal{R}}\|]. \tag{17}$$

Thus

$$\|\mathcal{F}(t, \mathcal{Z}(t)) - \mathcal{F}(\bar{t}, \overline{\mathcal{Z}(t)})\| \leq \frac{1-\varphi}{\mathcal{K}(\varphi)} [\|\mathcal{Z} - (\overline{\mathcal{Q}}, \overline{\mathcal{R}})\|], \tag{18}$$

which demonstrates the contraction property of $\mathcal{F}$. The definition of a closed subset $\mathcal{B}$ of $\mathcal{Z}$ is

$$\mathcal{B} = \{\mathcal{Z} \in \mathcal{Z} : \|\mathcal{Z}\| \leq r, \, r > 0\}. \tag{19}$$

For every $\mathcal{Z} \in \mathcal{B}$, we have the following argument that $\mathcal{G}$ is compact and continuous:

$$\begin{aligned} \|\mathcal{G}_1(\mathcal{Z})\| &\leq \max_{t\in[0,\mathbb{T}]} \frac{\varphi}{\Gamma(\varphi)\mathcal{K}(\varphi)} \int_0^t (t-y)^{\varphi-1} f(y, \mathcal{Z}(y))dy \\ &\leq \frac{\mathbb{T}^\varphi}{\Gamma(\varphi)\mathcal{K}(\varphi)} [C_f\|\mathcal{Q}\| + \mathcal{B}_f\|\mathcal{Q}\| + \mathcal{M}_f], \end{aligned} \tag{20}$$

$$\begin{aligned} \|\mathcal{G}_2(\mathcal{Z})\| &\leq \max_{t\in[0,\mathbb{T}]} \frac{\varphi}{\Gamma(\varphi)\mathcal{K}(\varphi)} \int_0^t (t-y)^{\varphi-1} g(y, \mathcal{Z}(y))dy \\ &\leq \frac{\mathbb{T}^\varphi}{\Gamma(\varphi)\mathcal{K}(\varphi)} [C_g\|\mathcal{R}\| + \mathcal{B}_g\|\mathcal{R}\| + \mathcal{M}_g]. \end{aligned} \tag{21}$$

Thus

$$\|\mathcal{G}(\mathcal{Z})\| \leq \mathbb{T}^\varphi \frac{[(C_1 + \mathcal{B}_1)r + \mathcal{M}_1]}{\mathcal{K}(\varphi)\Gamma(\varphi)} = \Delta, \tag{22}$$

where $C_1 = C_f + C_g$, $\mathcal{B}_1 = \mathcal{B}_f + \mathcal{B}_g$, $\mathcal{M}_1 = \mathcal{M}_f + \mathcal{M}_g$. Consequently, it is established that $\mathcal{G}$ is bounded. We will now show that $\mathcal{G}$ is equicontinuous. Considering that $t_1 < t_2 \in [0, \mathbb{T}]$,

$$\begin{aligned} |\mathcal{G}_1(\mathcal{Z})(t_2) - \mathcal{G}_1(\mathcal{Z})(t_1)| &= \frac{\varphi}{\Gamma(\varphi)\mathcal{K}(\varphi)} \Big| \int_0^{t_2} (t_2 - y)^{\varphi-1} f(\mathcal{Z}(y))dy \\ &\quad - \int_0^{t_1} (t_1 - y)^{\varphi-1} f(\mathcal{Z}(y))dy \Big| \\ &\leq \frac{\varphi}{\Gamma(\varphi)\mathcal{K}(\varphi)} [\int_0^{t_2} (t_2 - y)^{\varphi-1} \\ &\quad - \int_0^{t_1} (t_1 - y)^{\varphi-1}] ((C_f + \mathcal{B}_f)r + \mathcal{M}_f)dy \\ &\leq \frac{((C_f + \mathcal{B}_f)r + \mathcal{M}_f)}{\mathcal{K}(\varphi)\Gamma(\varphi)} [t_2^\varphi - t_1^\varphi], \end{aligned} \tag{23}$$

$$|\mathcal{G}_2(\mathcal{Z})(t_2) - \mathcal{G}_2(\mathcal{Z})(t_1)| \leq \frac{((C_g + \mathcal{B}_g)r + \mathcal{M}_g)}{\mathcal{K}(\varphi)\Gamma(\varphi)} [t_2^\varphi - t_1^\varphi]. \tag{24}$$

$\|\mathcal{G}_1(\mathcal{Z})(t_2) - \mathcal{G}_1(\mathcal{Z})(t_1)\| \longrightarrow 0$ as $t_1 \longrightarrow t_2$.
As a result, $\|\mathcal{G}(\mathcal{Z})(t_2) - \mathcal{G}(\mathcal{Z})(t_1)\| \longrightarrow 0$ as $t_1 \longrightarrow t_2$.
This proves that $\mathcal{G}$ is an equicontinuous operator. The Arzelà–Ascoli theorem then establishes that $\mathcal{G}$ is uniformly bounded and completely continuous. Hence, by Krasnoselskii's fixed-point theorem, the system has at least one solution. □

Theorem 3.2. Starting with the first assumption, our biomass system with the ABC derivative has a unique solution provided that

$$\left(\frac{1-\varphi}{\mathcal{K}(\varphi)} + \frac{\mathbb{T}^\varphi}{\mathcal{K}(\varphi)\Gamma(\varphi)}\right) 2\mathcal{L} < 1, \tag{25}$$

with $\max\{\mathcal{L}_f, \mathcal{L}_g\} = \mathcal{L}$.

Proof. Define the operator $\grave{\mathcal{P}} = (\mathcal{P}_1, \mathcal{P}_2) : \mathcal{Z} \to \mathcal{Z}$ as

$$\begin{aligned} \mathcal{P}_1\mathcal{Z}(t) &= \mathcal{Q}_0 + \frac{1-\varphi}{\mathcal{K}(\varphi)} f(t, \mathcal{Z}(t)) \\ &\quad + \frac{\varphi}{\Gamma(\varphi)\mathcal{K}(\varphi)} \int_0^t (t-y)^{\varphi-1} f(y, \mathcal{Z}(y))dy, \end{aligned} \tag{26}$$

$$\begin{aligned} \mathcal{P}_2\mathcal{Z}(t) &= \mathcal{R}_0 + \frac{1-\varphi}{\mathcal{K}(\varphi)} g(t, \mathcal{Z}(t)) \\ &\quad + \frac{\varphi}{\Gamma(\varphi)\mathcal{K}(\varphi)} \int_0^t (t-y)^{\varphi-1} g(y, \mathcal{Z}(y))dy. \end{aligned} \tag{27}$$

Now, we take $\mathcal{Z} = (\mathcal{Q}, \mathcal{R})$ and $\overline{\mathcal{Z}} = (\overline{\mathcal{Q}}, \overline{\mathcal{R}})$. For the first component, the Lipschitz condition (10) controls both the local term and the integral term, so

$$\begin{aligned} &\|\mathcal{P}_1(\mathcal{Z}) - \mathcal{P}_1(\overline{\mathcal{Z}})\| \\ &\leq \frac{1-\varphi}{\mathcal{K}(\varphi)} \mathcal{L}_f \|\mathcal{Z} - \overline{\mathcal{Z}}\| \\ &+ \frac{\varphi}{\Gamma(\varphi)\mathcal{K}(\varphi)} \max_{t\in[0,\mathbb{T}]} \int_0^t (t-y)^{\varphi-1} |f(y, \mathcal{Z}(y)) - f(y, \overline{\mathcal{Z}}(y))|dy \\ &\leq \left(\frac{1-\varphi}{\mathcal{K}(\varphi)} + \frac{\mathbb{T}^\varphi}{\mathcal{K}(\varphi)\Gamma(\varphi)}\right) \mathcal{L}_f [\|\mathcal{Q} - \overline{\mathcal{Q}}\| + \|\mathcal{R} - \overline{\mathcal{R}}\|], \end{aligned} \tag{28}$$

where the integral term is estimated by evaluating $\int_0^t (t - y)^{\varphi-1} dy = t^\varphi/\varphi \leq \mathbb{T}^\varphi/\varphi$ and using $\Gamma(\varphi + 1) = \varphi\Gamma(\varphi)$. Similarly, for the second component,

$$\|\mathcal{P}_2(\mathcal{Z}) - \mathcal{P}_2(\overline{\mathcal{Z}})\| \leq \left(\frac{1-\varphi}{\mathcal{K}(\varphi)} + \frac{\mathbb{T}^\varphi}{\mathcal{K}(\varphi)\Gamma(\varphi)}\right)$$

$$\mathcal{L}_g[\|\mathcal{Q}-\overline{\mathcal{Q}}\|+\|\mathcal{R}-\overline{\mathcal{R}}\|], \tag{29}$$

Combining equations (36) and (44) and recalling $\mathcal{L} = \max\{\mathcal{L}_f, \mathcal{L}_g\}$, we obtain

$$\|\mathcal{P}(\mathcal{Z})-\mathcal{P}(\overline{\mathcal{Z}})\| \le \left(\frac{1-\varphi}{\mathcal{K}(\varphi)}+\frac{\mathbb{T}^{\varphi}}{\mathcal{K}(\varphi)\Gamma(\varphi)}\right)2\mathcal{L}\|\mathcal{Z}-\overline{\mathcal{Z}}\|. \tag{30}$$

Therefore $\mathcal{P}$ is a contraction whenever the sufficient condition (25) holds. According to the Banach contraction theorem, there is a unique solution for the entire system. We then present Ulam-Hyers stability results. □

Theorem 3.3. If the spectral radius of the resulting matrix is strictly less than one, then the analyzed model's solution is Ulam-Hyers stable.

$$\begin{bmatrix} a & a \\ b & b \end{bmatrix} \tag{31}$$

The stability condition is $|a+b|<1$, where

$$a=\left(\frac{(1-\varphi)}{\mathcal{K}(\varphi)}+\frac{\mathbb{T}^{\varphi}}{\mathcal{K}(\varphi)\Gamma(\varphi)}\right)\mathcal{L}_f, \tag{32}$$

$$b=\left(\frac{(1-\varphi)}{\mathcal{K}(\varphi)}+\frac{\mathbb{T}^{\varphi}}{\mathcal{K}(\varphi)\Gamma(\varphi)}\right)\mathcal{L}_g. \tag{33}$$

Proof. Let $\mathcal{Z}$ be any model solution, and let $\overline{\mathcal{Z}}$ be the model unique solution, such that

$$\|\mathcal{Z}-\overline{\mathcal{Z}}\| \le \begin{bmatrix} a & a \\ b & b \end{bmatrix}\begin{bmatrix} \|\mathcal{Q}-\overline{\mathcal{Q}}\| \\ \|\mathcal{R}-\overline{\mathcal{R}}\| \end{bmatrix}. \tag{34}$$

Since the eigenvalues of the matrix are 0 and $a+b$, the spectral radius is $|a+b|$, and the condition $|a+b|<1$ ensures the system is stable. □

4. Fractional operator ABC in a mathematical model

In this section, we analyze the proposed operator for the biomass model for existence, uniqueness and stability of the system.

Theorem 4.1. The solution $(\mathcal{Q}(t),\mathcal{R}(t))$ of system (7) with initial data $(\mathcal{Q}(0),\mathcal{R}(0)) \in \mathcal{R}^2_+$ remains non-negative for all $t \ge 0$.

Proof. Evaluating the vector field of (7) on the boundary planes of the positive orthant $\mathcal{R}^2_+$, we obtain

$${}^{ABC}D^{\varphi}_t\mathcal{Q}\big|_{\mathcal{Q}=0}=0, \qquad {}^{ABC}D^{\varphi}_t\mathcal{R}\big|_{\mathcal{R}=0}=0. \tag{35}$$

Since the ABC derivative on each boundary plane is non-negative for non-negative $\mathcal{R}$ and $\mathcal{Q}$ respectively, no trajectory starting in $\mathcal{R}^2_+$ can cross either coordinate axis. Hence $\mathcal{R}^2_+$ is a positively invariant set, and the solution remains non-negative for all $t \ge 0$. □

4.1. Positivity and boundedness

In this subsection we establish positivity and boundedness directly for the ABC system (7). We use the following fractional comparison principle.

Lemma 4.1. [29] Let $\phi \in (0,1]$ and let $u : [0,T] \to \mathbb{R}$ be continuous. If ${}^{ABC}D^{\phi}_t u(t) \ge 0$ for all $t \in (0,T]$, then $u(t) \ge u(0)$ for all $t \in [0,T]$. In particular, if $u(0) \ge 0$, then $u(t) \ge 0$ for all $t \in [0,T]$.

Proof. From Definition 2.2, the ABC integral of ${}^{ABC}D^{\phi}_t u$ is

$${}^{ABC}I^{\phi}_t[{}^{ABC}D^{\phi}_t u](t) = u(t)-u(0).$$

Since ${}^{ABC}D^{\phi}_t u(t) \ge 0$ and the ABC integral operator is positivity preserving, it follows that $u(t)-u(0) \ge 0$, i.e. $u(t) \ge u(0)$. □

Positivity. Consider the $\mathcal{R}$-equation of system (7), which can be rewritten as

$${}^{ABC}D^{\varphi}_t\mathcal{R} = \mathcal{R}\,\Psi_1(t,\mathcal{Q},\mathcal{R}), \tag{36}$$

where

$$\Psi_1(t,\mathcal{Q},\mathcal{R}) = s\Big(1-\frac{\mathcal{R}}{\mathcal{L}}\Big)+\beta_1\mathcal{Q}-\beta_2\mathcal{Q}^2. \tag{37}$$

Since Ψ_1 is continuous and $\mathcal{Q},\mathcal{R}$ are continuous on $[0,T]$, Ψ_1 is bounded on every compact subset of $\mathcal{R}^2_+$. Let

$$M_1 = \max_{[0,T]\times\mathcal{B}_r}|\Psi_1(t,\mathcal{Q},\mathcal{R})|, \tag{38}$$

where $\mathcal{B}_r$ is any closed ball containing the trajectory. Then

$${}^{ABC}D^{\varphi}_t\mathcal{R} + M_1\mathcal{R} \ge 0. \tag{39}$$

Multiplying by $E_{\varphi}[\frac{\varphi}{1-\varphi}t^{\varphi}]$ and using the product rule for the ABC operator, we obtain

$${}^{ABC}D^{\varphi}_t\Big[\mathcal{R}(t)\,E_{\varphi}\Big[\tfrac{\varphi}{1-\varphi}t^{\varphi}\Big]\Big] \ge 0. \tag{40}$$

By Lemma 4.1,

$$\mathcal{R}(t)\,E_{\varphi}\Big[\tfrac{\varphi}{1-\varphi}t^{\varphi}\Big] \ge \mathcal{R}(0) \ge 0, \tag{41}$$

hence $\mathcal{R}(t) \ge 0$ for all $t \in [0,T]$. Similarly, writing the $\mathcal{Q}$-equation as

$${}^{ABC}D^{\varphi}_t\mathcal{Q} = \mathcal{Q}\,\Psi_2(t,\mathcal{Q},\mathcal{R}), \tag{42}$$

with

$$\Psi_2(t,\mathcal{Q},\mathcal{R}) = r\Big(1-\frac{\mathcal{Q}}{\mathcal{K}}\Big)-\alpha_1\mathcal{R}-\alpha_2\mathcal{R}\mathcal{Q}-q\mathcal{E}, \tag{43}$$

and repeating the same argument yields $\mathcal{Q}(t) \ge 0$ for all $t \in [0,T]$. Therefore $\mathcal{R}^2_+$ is positively invariant.

Boundedness.

Consider first the $\mathcal{R}$-equation. From (7),

$${}^{ABC}D^{\varphi}_t\mathcal{R} = s\mathcal{R}\Big(1-\frac{\mathcal{R}}{\mathcal{L}}\Big)+\beta_1\mathcal{R}\mathcal{Q}-\beta_2\mathcal{R}\mathcal{Q}^2. \tag{44}$$

Since $\mathcal{Q}(t) \geq 0$ and $\mathcal{R}(t) \geq 0$ on $\mathcal{R}_+^2$, and since the term $-\beta_2 \mathcal{R}\mathcal{Q}^2$ is non-positive, we obtain the fractional differential inequality

$$^{ABC}D_t^{\varphi}\mathcal{R} \leq s\mathcal{R}\Big(1 - \frac{\mathcal{R}}{\mathcal{L}}\Big) + \beta_1 \mathcal{R}\mathcal{Q}. \tag{45}$$

To close the estimate without assuming boundedness of $\mathcal{Q}$, we use the fact that $\mathcal{Q}$ is continuous on the compact interval $[0, T]$, so $\mathcal{Q}(t) \leq \mathcal{Q}_{\max}$ for some finite constant $\mathcal{Q}_{\max}$ depending only on T and the initial data. Then

$$^{ABC}D_t^{\varphi}\mathcal{R} \leq \mathcal{R}\Big(s + \beta_1 \mathcal{Q}_{\max} - \frac{s}{\mathcal{L}}\mathcal{R}\Big). \tag{46}$$

By the fractional comparison principle, $\mathcal{R}$ is bounded above by the solution of the associated Bernoulli-type ABC equation, which remains finite on $[0, T]$. Hence there exists $\mathcal{R}_{\max} > 0$ such that

$$0 \leq \mathcal{R}(t) \leq \mathcal{R}_{\max}, \qquad \forall\, t \in [0, T]. \tag{47}$$

Now consider the $\mathcal{Q}$-equation. Using $\mathcal{R}(t) \leq \mathcal{R}_{\max}$ and $\mathcal{Q}(t) \geq 0$,

$$\begin{aligned} ^{ABC}D_t^{\varphi}\mathcal{Q} &= r\mathcal{Q}\Big(1 - \frac{\mathcal{Q}}{\mathcal{K}}\Big) - \alpha_1 \mathcal{R}\mathcal{Q} - \alpha_2 \mathcal{R}\mathcal{Q}^2 - q\mathcal{E}\mathcal{Q} \\ &\leq r\mathcal{Q}\Big(1 - \frac{\mathcal{Q}}{\mathcal{K}}\Big) - q\mathcal{E}\mathcal{Q} \\ &= \mathcal{Q}\Big(r - q\mathcal{E} - \frac{r}{\mathcal{K}}\mathcal{Q}\Big). \end{aligned} \tag{48}$$

Again by the fractional comparison principle, $\mathcal{Q}$ is bounded above by the solution of the corresponding ABC logistic-type equation, which is finite on $[0, T]$. Therefore there exists $\mathcal{Q}_{\max} > 0$ such that

$$0 \leq \mathcal{Q}(t) \leq \mathcal{Q}_{\max}, \qquad \forall\, t \in [0, T]. \tag{49}$$

Combining (47) and (49), the solution $(\mathcal{Q}(t), \mathcal{R}(t))$ of the ABC system (7) is positive and bounded in $\mathcal{R}_+^2$ for all $t \in [0, T]$.

4.2. Equilibrium points of the system

Setting the left-hand sides of the system (7) to zero yields the equilibrium equations

$$\begin{cases} r\mathcal{Q}(1 - \frac{\mathcal{Q}}{\mathcal{K}}) - \alpha_1 \mathcal{R}\mathcal{Q} - \alpha_2 \mathcal{R}\mathcal{Q}^2 - q\mathcal{E}\mathcal{Q} &= 0, \\ s\mathcal{R}(1 - \frac{\mathcal{R}}{\mathcal{L}}) + \beta_1 \mathcal{R}\mathcal{Q} - \beta_2 \mathcal{R}\mathcal{Q}^2 &= 0. \end{cases} \tag{50}$$

The system is two-dimensional in $(\mathcal{Q}, \mathcal{R})$. The population-free equilibria are obtained by setting $\mathcal{Q} = 0$, which gives

$$E_0 = (0, 0), \qquad E_1 = (0, \mathcal{L}). \tag{51}$$

For a coexistence equilibrium, we consider $\mathcal{Q} > 0$ and $\mathcal{R} > 0$. Dividing the first equation of (61) by $\mathcal{Q}$ and the second by $\mathcal{R}$ gives

$$r\Big(1 - \frac{\mathcal{Q}}{\mathcal{K}}\Big) - \alpha_1 \mathcal{R} - \alpha_2 \mathcal{R}\mathcal{Q} - q\mathcal{E} = 0, \tag{52}$$

$$s\Big(1 - \frac{\mathcal{R}}{\mathcal{L}}\Big) + \beta_1 \mathcal{Q} - \beta_2 \mathcal{Q}^2 = 0. \tag{53}$$

Equation (63) is linear in $\mathcal{R}$; solving for $\mathcal{R}$ gives

$$\mathcal{R} = \frac{r(1 - \mathcal{Q}/\mathcal{K}) - q\mathcal{E}}{\alpha_1 + \alpha_2 \mathcal{Q}}. \tag{54}$$

Substituting (68) into (64) yields a scalar equation for $\mathcal{Q}$, which determines the coexistence equilibrium $E^* = (\mathcal{Q}^*, \mathcal{R}^*)$ with $\mathcal{R}^*$ given by (68). The coexistence equilibrium is biologically feasible whenever $\mathcal{Q}^* > 0$ and $\mathcal{R}^* > 0$.

4.3. Existence, stability and uniqueness theory

In this section of the article, the ABC operator is used to discuss the stability, uniqueness and existence of the model.

4.3.1. Global stability via a fractional Lyapunov function

Before proceeding, we state important lemmas for the fractional Lyapunov stability.

Lemma 4.2. Let $\mathbb{L} : [0, \infty) \to \mathbb{R}$ be a continuously differentiable, positive-definite function, and let Ω be a positively invariant compact set of the ABC system (7). If

$$^{ABC}D_t^{\varphi}\mathbb{L}(t) \leq 0, \quad \text{for all } t \geq 0, \quad \text{and all } (\mathcal{Q}, \mathcal{R}) \in \Omega, \tag{55}$$

if the largest invariant subset of $\{(\mathcal{Q}, \mathcal{R}) \in \Omega : {}^{ABC}D_t^{\varphi}\mathbb{L} = 0\}$ is the equilibrium E^*, then E^* is globally asymptotically stable in Ω [30].

Lemma 4.3. [30] Let $\varphi \in (0, 1)$ and let $G(t)$ be a positive-valued and continuously differentiable function on $[0, T]$. Then, for all $t \in [0, T)$, the ABC fractional derivative of order φ of the Volterra-type function satisfies

$$^{ABC}\mathcal{D}_t^{\varphi}\Big(G(t) - G^* - G^* \ln \frac{G(t)}{G^*}\Big) \leq \Big(1 - \frac{G^*}{G(t)}\Big)\,{}^{ABC}\mathcal{D}_t^{\varphi}G(t), \tag{56}$$

for any positive constant $G^* \in \mathbb{R}^+$.

We establish the global asymptotic stability of the coexistence equilibrium $E^* = (\mathcal{Q}^*, \mathcal{R}^*)$ under explicit parameter conditions.

Theorem 4.2. Assume that the coexistence equilibrium $E^* = (\mathcal{Q}^*, \mathcal{R}^*)$ exists with $\mathcal{Q}^* > 0$, $\mathcal{R}^* > 0$, and that the parameter conditions

$$C_1 : \quad r + \alpha_1 \mathcal{R} + \alpha_2 \mathcal{R}\mathcal{Q} + q\mathcal{E} > \frac{2r\mathcal{Q}^*}{\mathcal{K}}, \tag{57}$$

$$C_2 : \quad s + \beta_1 \mathcal{Q} + \mathcal{Q}^2\beta_2 > \frac{2s\mathcal{R}^*}{\mathcal{L}}, \tag{58}$$

hold. Then E^* is globally asymptotically stable in Γ, where $\Gamma \subset \mathcal{R}_+^2$ is the positively invariant compact set defined in Section 4.1, containing the coexistence equilibrium E^* in its interior.

Proof. The Lyapunov function is chosen in the standard Volterra form

$$\mathbb{L}(\mathcal{Q},\mathcal{R}) = \left(\mathcal{Q}-\mathcal{Q}^*-\mathcal{Q}^*\ln\frac{\mathcal{Q}}{\mathcal{Q}^*}\right)+\left(\mathcal{R}-\mathcal{R}^*-\mathcal{R}^*\ln\frac{\mathcal{R}}{\mathcal{R}^*}\right). \quad (59)$$

This function is positive definite on $\Gamma\setminus\{E^*\}$ and vanishes only at $E^*=(\mathcal{Q}^*,\mathcal{R}^*)$. According to Lemma 4.3, its ABC fractional derivative satisfies

$${}^{ABC}D_t^{\varphi}\mathbb{L} \le \left(1-\frac{\mathcal{Q}^*}{\mathcal{Q}}\right){}^{ABC}D_t^{\varphi}\mathcal{Q}+\left(1-\frac{\mathcal{R}^*}{\mathcal{R}}\right){}^{ABC}D_t^{\varphi}\mathcal{R}. \quad (60)$$

Substituting (7) into (60) gives

$$\begin{aligned}{}^{ABC}D_t^{\varphi}\mathbb{L} \le{}& \Big(\frac{\mathcal{Q}-\mathcal{Q}^*}{\mathcal{Q}}\Big)\Big(r\mathcal{Q}(1-\frac{\mathcal{Q}}{\mathcal{K}})-\alpha_1\mathcal{R}\mathcal{Q}-\alpha_2\mathcal{R}\mathcal{Q}^2-q\mathcal{E}\mathcal{Q}\Big)\\ &+\Big(\frac{\mathcal{R}-\mathcal{R}^*}{\mathcal{R}}\Big)\Big(s\mathcal{R}(1-\frac{\mathcal{R}}{\mathcal{L}})+\beta_1\mathcal{R}\mathcal{Q}-\beta_2\mathcal{R}\mathcal{Q}^2\Big). \quad (61)\end{aligned}$$

Using the equilibrium relations (52)–(53) and expanding around E^*, we obtain

$${}^{ABC}D_t^{\varphi}\mathbb{L} \le \Phi_1-\Phi_2, \quad (62)$$

where the sign-definite and sign-indefinite terms are separated as

$$\begin{aligned}\Phi_1 =& \frac{r(\mathcal{Q}-\mathcal{Q}^*)^2}{\mathcal{Q}}+\frac{\mathcal{R}^*\alpha_1(\mathcal{Q}-\mathcal{Q}^*)^2}{\mathcal{Q}}+\frac{\mathcal{R}^*\alpha_2(\mathcal{Q}-\mathcal{Q}^*)^3}{\mathcal{Q}}\\ &+\frac{s(\mathcal{R}-\mathcal{R}^*)^2}{\mathcal{R}}+\frac{\mathcal{Q}\beta_1(\mathcal{R}-\mathcal{R}^*)^2}{\mathcal{R}}+\frac{2\mathcal{Q}\mathcal{Q}^*\beta_2(\mathcal{R}-\mathcal{R}^*)^2}{\mathcal{R}}, \quad (63)\end{aligned}$$

$$\begin{aligned}\Phi_2 =& \frac{r(\mathcal{Q}-\mathcal{Q}^*)^2}{\mathcal{Q}\mathcal{K}}+\frac{\mathcal{R}\alpha_1(\mathcal{Q}-\mathcal{Q}^*)^2}{\mathcal{Q}}+\frac{\mathcal{R}\alpha_2(\mathcal{Q}-\mathcal{Q}^*)^3}{\mathcal{Q}}\\ &+\frac{q\mathcal{E}(\mathcal{Q}-\mathcal{Q}^*)^2}{\mathcal{Q}}+\frac{s(\mathcal{R}-\mathcal{R}^*)^3}{\mathcal{R}\mathcal{L}}+\frac{\mathcal{Q}^*\beta_1(\mathcal{R}-\mathcal{R}^*)^2}{\mathcal{R}}\\ &+\frac{\mathcal{Q}^2\beta_2(\mathcal{R}-\mathcal{R}^*)^2}{\mathcal{R}}+\frac{\mathcal{Q}^{*2}\beta_2(\mathcal{R}-\mathcal{R}^*)^2}{\mathcal{R}}. \quad (64)\end{aligned}$$

To obtain a sufficient condition for $\Phi_1-\Phi_2\le 0$, we group the terms in Φ_1 and Φ_2 by powers of $(\mathcal{Q}-\mathcal{Q}^*)$ and $(\mathcal{R}-\mathcal{R}^*)$. After collecting terms and using the equilibrium relations, the leading quadratic contribution can be written as

$$\begin{aligned}\Phi_1-\Phi_2 \le{}& -\Big[\frac{r}{\mathcal{K}}-\frac{2r\mathcal{Q}^*}{\mathcal{K}\mathcal{Q}}-\alpha_1\frac{\mathcal{R}}{\mathcal{Q}}-\alpha_2\frac{\mathcal{R}\mathcal{Q}}{\mathcal{Q}}-\frac{q\mathcal{E}}{\mathcal{Q}}\Big](\mathcal{Q}-\mathcal{Q}^*)^2\\ &-\Big[\frac{s}{\mathcal{L}}-\frac{2s\mathcal{R}^*}{\mathcal{L}\mathcal{R}}-\beta_1\frac{\mathcal{Q}}{\mathcal{R}}-\beta_2\frac{\mathcal{Q}^2}{\mathcal{R}}\Big](\mathcal{R}-\mathcal{R}^*)^2. \quad (65)\end{aligned}$$

Therefore, $\Phi_1-\Phi_2\le 0$ whenever the parameter conditions (57)–(58) hold, i.e.

$$r+\alpha_1\mathcal{R}+\alpha_2\mathcal{R}\mathcal{Q}+q\mathcal{E} \ge \frac{2r\mathcal{Q}^*}{\mathcal{K}}, \quad (66)$$

$$s+\beta_1\mathcal{Q}+\beta_2\mathcal{Q}^2 \ge \frac{2s\mathcal{R}^*}{\mathcal{L}}. \quad (67)$$

Consequently ${}^{ABC}D_t^{\varphi}\mathbb{L}\le 0$ on Γ, with equality holding only when $\mathcal{Q}=\mathcal{Q}^*$ and $\mathcal{R}=\mathcal{R}^*$. The largest compact invariant set in

$$\Big\{(\mathcal{Q},\mathcal{R})\in\Gamma;\ {}^{ABC}D_t^{\varphi}\mathbb{L}=0\Big\} \quad (68)$$

is therefore the singleton $\{E^*\}$. By Lemma 4.2 and LaSalle's invariance principle, the coexistence equilibrium E^* is globally asymptotically stable in Γ. □

4.4. Extension to the fractal-fractional (ABR) setting

The main model (7) is formulated with the ABC operator. In this subsection we show that the existence and uniqueness results established in Section 3 extend to the broader fractal-fractional (ABR) setting. This extension is presented solely to demonstrate the robustness of the results under a more general operator and does not alter the ABC model analyzed above.

Definition 4.3. [9] Let $\psi\in H^1(0,T)$ and let $\varphi\in(0,1]$ and $\zeta>0$. The ABR fractal-fractional derivative of order (φ,ζ) is defined by

$${}^{ABR}_{0}D_t^{\varphi,\zeta}\psi(t) = \frac{\mathcal{K}(\varphi)}{1-\varphi}\frac{d}{dt^{\zeta}}\int_0^t E_{\varphi}\Big[\frac{-\varphi}{1-\varphi}(t-y)^{\varphi}\Big]\psi(y)dy, \quad (69)$$

where $\frac{d}{dt^{\zeta}}$ denotes the fractal derivative of order ζ, and $\mathcal{K}(\varphi)$ is the normalization function introduced in Section 2 with $\mathcal{K}(0)=\mathcal{K}(1)=1$. The fractal derivative is defined, for differentiable ψ, by

$$\frac{d\psi}{dt^{\zeta}}(t) = t^{1-\zeta}\frac{d\psi}{dt}(t). \quad (70)$$

Applying (69)–(70) to system (7), the ABR fractal-fractional formulation of the model is

$$\begin{cases}{}^{ABR}_{0}D_t^{\varphi,\zeta}\mathcal{Q} = t^{1-\zeta}\,\mathcal{Z}(\mathcal{K}_1),\\ {}^{ABR}_{0}D_t^{\varphi,\zeta}\mathcal{R} = t^{1-\zeta}\,\mathcal{Y}(\mathcal{K}_1),\end{cases} \quad (71)$$

where $\mathcal{K}_1=(t,\mathcal{Q},\mathcal{R})$ and

$$\begin{cases}\mathcal{Z}(\mathcal{K}_1) = r\mathcal{Q}(1-\frac{\mathcal{Q}}{\mathcal{K}})-\alpha_1\mathcal{R}\mathcal{Q}-\alpha_2\mathcal{R}\mathcal{Q}^2-q\mathcal{E}\mathcal{Q},\\ \mathcal{Y}(\mathcal{K}_1) = s\mathcal{R}(1-\frac{\mathcal{R}}{\mathcal{L}})+\beta_1\mathcal{R}\mathcal{Q}-\beta_2\mathcal{R}\mathcal{Q}^2.\end{cases} \quad (72)$$

We can write the system as

$$\begin{cases}{}^{ABR}_{0}D_t^{\varphi}\Upsilon(t) = t^{1-\zeta}\Psi(t,\Upsilon(t)),\\ \Upsilon(0)=\Upsilon_0.\end{cases} \quad (73)$$

Since $\zeta\in(0,1)$, the factor $t^{1-\zeta}$ is continuous on $[0,\mathbb{T}]$ and vanishes at $t=0$; hence no singularity arises at the initial point. By replacing ${}^{ABR}_{0}D_0^{\varphi,\zeta}$ with ${}^{ABC}D_t^{\varphi}$ and applying the fractal-fractional integral, we obtain

$$\begin{aligned}\Upsilon(t) = \Upsilon(0)&+\frac{t^{1-\zeta}(1-\varphi)}{\mathcal{K}(\varphi)}\Psi(t,\Upsilon(t))\\ &+\frac{\varphi}{\mathcal{K}(\varphi)\Gamma(\varphi)}\int_0^t y^{1-\zeta}(t-y)^{\varphi-1}\Psi(y,\Upsilon(y))dy, \quad (74)\end{aligned}$$

where

$$\Upsilon(t)=\begin{pmatrix}\mathcal{Q}(t)\\ \mathcal{R}(t)\end{pmatrix},\qquad \Upsilon(0)=\begin{pmatrix}\mathcal{Q}(0)\\ \mathcal{R}(0)\end{pmatrix},\qquad \Psi(t,\Upsilon(t))=\begin{pmatrix}\mathcal{Z}(\mathcal{K}_1)\\ \mathcal{Y}(\mathcal{K}_1)\end{pmatrix}. \quad (75)$$

The existence theory makes use of the Banach space

$$\mathbb{B}=\mathcal{X}\times\mathcal{X},\qquad \mathcal{X}=C([0,\mathbb{T}],\mathbb{R}), \quad (76)$$

equipped with the norm

$$\|\Upsilon\|_{\mathbb{B}} = \|\mathcal{Q}\|_{\infty}+\|\mathcal{R}\|_{\infty} = \max_{t\in[0,\mathbb{T}]}|\mathcal{Q}(t)|+\max_{t\in[0,\mathbb{T}]}|\mathcal{R}(t)|. \quad (77)$$

Because $t^{1-\zeta}$ is continuous on the closed interval $[0,\mathbb{T}]$ and the kernel $(t-y)^{\varphi-1}$ is integrable for $\varphi\in(0,1)$, the operator below is well defined on $\mathbb{B}$. Define $\mathfrak{I}:\mathbb{B}\to\mathbb{B}$ as

$$\mathfrak{I}(\Upsilon)(t) = \Upsilon(0) + \frac{t^{1-\zeta}(1-\varphi)}{\mathcal{K}(\varphi)}\Psi(t,\Upsilon(t)) + \frac{\varphi}{\mathcal{K}(\varphi)\Gamma(\varphi)}\int_0^t y^{1-\zeta}(t-y)^{\varphi-1}\Psi(y,\Upsilon(y))dy. \quad (78)$$

Assume that the given requirements are satisfied by the nonlinear term $\Psi(t,\Upsilon(t))$.

- For each $\Upsilon\in\mathbb{B}$, there exist constants $\mathcal{A}_\Psi$ and $\mathcal{P}_\Psi$ such that

$$|\Psi(t,\Upsilon(t))|\le\mathcal{A}_\Psi|\Upsilon(t)|+\mathcal{P}_\Psi, \quad (79)$$

- For each $\Upsilon,\overline{\Upsilon}\in\mathbb{B}$, there exists a constant $\mathcal{K}_\Psi>0$ such that

$$|\Psi(t,\Upsilon(t))-\Psi(t,\overline{\Upsilon}(t))|\le\mathcal{K}_\Psi|\Upsilon(t)-\overline{\Upsilon}(t)|. \quad (80)$$

Theorem 4.4. Let $\Psi:[0,\mathbb{T}]\times\mathbb{B}\to\mathbb{R}$ be a continuous function. If condition (79) holds and the operator $\mathfrak{I}$ in (78) satisfies the contraction condition

$$\frac{\mathbb{T}^{1-\zeta}(1-\varphi)}{\mathcal{K}(\varphi)}\mathcal{K}_\Psi+\frac{\varphi\,\mathbb{T}^{\varphi-\zeta}}{\mathcal{K}(\varphi)\Gamma(\varphi)}\mathcal{K}_\Psi<1, \quad (81)$$

then the fractal-fractional system (73) has a unique solution in $\mathbb{B}$.

Proof. We show that $\mathfrak{I}$ maps a closed ball $\mathcal{B}_r=\{\Upsilon\in\mathbb{B}:\|\Upsilon\|_{\mathbb{B}}\le r\}$ into itself and is a contraction; the result then follows from the Banach contraction theorem.

(i). Boundedness of $\mathfrak{I}$. For $\Upsilon\in\mathcal{B}_r$, using (79),

$$\|\mathfrak{I}(\Upsilon)\|_{\mathbb{B}}\le\Upsilon(0)+\frac{\mathbb{T}^{1-\zeta}(1-\varphi)}{\mathcal{K}(\varphi)}(\mathcal{A}_\Psi r+\mathcal{P}_\Psi)+\frac{\varphi\mathbb{T}^{\varphi-\zeta}}{\mathcal{K}(\varphi)\Gamma(\varphi)}(\mathcal{A}_\Psi r+\mathcal{P}_\Psi)\mathcal{L}(\varphi,\zeta), \quad (82)$$

where $\mathcal{L}(\varphi,\zeta)$ is a bounded constant depending only on φ and ζ. Choosing r sufficiently large makes $\|\mathfrak{I}(\Upsilon)\|_{\mathbb{B}}\le r$, so $\mathfrak{I}$ maps $\mathcal{B}_r$ into itself.

(ii). Contraction of $\mathfrak{I}$. For $\Upsilon,\overline{\Upsilon}\in\mathbb{B}$, using (80),

$$\|\mathfrak{I}(\Upsilon)-\mathfrak{I}(\overline{\Upsilon})\|_{\mathbb{B}}\le\frac{\mathbb{T}^{1-\zeta}(1-\varphi)}{\mathcal{K}(\varphi)}\mathcal{K}_\Psi\|\Upsilon-\overline{\Upsilon}\|_{\mathbb{B}}+\frac{\varphi\,\mathbb{T}^{\varphi-\zeta}}{\mathcal{K}(\varphi)\Gamma(\varphi)}\mathcal{K}_\Psi\|\Upsilon-\overline{\Upsilon}\|_{\mathbb{B}}. \quad (83)$$

Under condition (81), the right-hand side is strictly smaller than $\|\Upsilon-\overline{\Upsilon}\|_{\mathbb{B}}$, so $\mathfrak{I}$ is a contraction. By the Banach contraction theorem, (73) has a unique solution in $\mathbb{B}$.

(iii). Equicontinuity. For $t_1<t_2\in[0,\mathbb{T}]$ and $\Upsilon\in\mathcal{B}_r$,

$$\|\mathfrak{I}(\Upsilon)(t_2)-\mathfrak{I}(\Upsilon)(t_1)\|_{\mathbb{B}}\le\Big|\frac{t_2^{1-\zeta}-t_1^{1-\zeta}}{\mathcal{K}(\varphi)}\Big|1-\varphi\Big|(\mathcal{A}_\Psi r+\mathcal{P}_\Psi)+\frac{\varphi}{\mathcal{K}(\varphi)\Gamma(\varphi)}(\mathcal{A}_\Psi r+\mathcal{P}_\Psi)M, \quad (84)$$

where

$$M=\Big|\int_0^{t_2}y^{1-\zeta}(t_2-y)^{\varphi-1}dy-\int_0^{t_1}y^{1-\zeta}(t_1-y)^{\varphi-1}dy\Big|.$$

Since $1-\zeta>0$ for $\zeta\in(0,1)$, the map $t\mapsto t^{1-\zeta}$ is continuous on $[0,\mathbb{T}]$; hence $t_2^{1-\zeta}-t_1^{1-\zeta}\to0$ as $t_1\to t_2$. As $t_1\to t_2$, the right-hand side tends to zero, so $\mathfrak{I}$ is equicontinuous. By the Arzelà–Ascoli theorem, $\mathfrak{I}$ is completely continuous. Together with the contraction estimate (83), this establishes the existence of a unique solution of (73) in $\mathbb{B}$. □

According to theorem 4.3, the fractal-fractional (ABR) system (73) has the same existence and uniqueness properties as the ABC system discussed in section 3. Thus, even when the more generic fractal-fractional operator is used, the results remain consistent. The fractal-fractional system (73) is only used to prove the prior assumption. All other results in this section refer to the ABC system (7).

5. Generalized form of proposed system for numerical solution

In the following section, the ABC fractal operator and Lagrangian piecewise interpolation [24] are used to build the numerical method for the proposed model. We have system

$$\begin{cases}{}^{ABC}D_t^{\varphi}\mathcal{Q}=r\mathcal{Q}(1-\frac{\mathcal{Q}}{\mathcal{K}})-\alpha_1\mathcal{R}\mathcal{Q}-\alpha_2\mathcal{R}\mathcal{Q}^2-q\mathcal{E}\mathcal{Q},\\ {}^{ABC}D_t^{\varphi}\mathcal{R}=s\mathcal{R}(1-\frac{\mathcal{R}}{\mathcal{L}})+\beta_1\mathcal{R}\mathcal{Q}-\beta_2\mathcal{R}\mathcal{Q}^2.\end{cases} \quad (85)$$

We can write as

$$\mathcal{Q}=\mathcal{Q}(0)+\frac{t^{1-\zeta}(1-\varphi)}{\mathcal{K}(\varphi)}\mathcal{L}_1(\mathcal{K}_1)+\frac{\varphi}{\mathcal{K}(\varphi)\Gamma(\varphi)}\int_0^t y^{1-\zeta}(t-y)^{\varphi-1}\mathcal{L}_1(\mathcal{K}_2)dy, \quad (86)$$

$$\mathcal{R}(t)=\mathcal{R}(0)+\frac{t^{1-\zeta}(1-\varphi)}{\mathcal{K}(\varphi)}\mathcal{L}_2(\mathcal{K}_1)+\frac{\varphi}{\mathcal{K}(\varphi)\Gamma(\varphi)}\int_0^t y^{1-\zeta}(t-y)^{\varphi-1}\mathcal{L}_2(\mathcal{K}_2)dy, \quad (87)$$

where $\mathcal{K}_1=(t,\mathcal{Q},\mathcal{R})$, $\mathcal{K}_2=(y,\mathcal{Q},\mathcal{R})$, and

$$\Phi=y^{1-\zeta}(t-y)^{\varphi-1}. \quad (88)$$

The kernel exponent is $\varphi-1$ in both equations, consistent with the ABC kernel of order φ; the factor $y^{1-\zeta}$ originates from the fractal derivative of order ζ. Now, at $t=t_{x+1}$, we get

$$\mathcal{Q}^{x+1}=\mathcal{Q}^0+\frac{t_x^{1-\zeta}(1-\varphi)}{\mathcal{K}(\varphi)}\mathcal{L}_1(t_x,\mathcal{Q}^x,\mathcal{R}^x)+\frac{\varphi}{\mathcal{K}(\varphi)\Gamma(\varphi)}\int_0^{t_{x+1}}y^{1-\zeta}(t_{x+1}-y)^{\varphi-1}\mathcal{L}_1(y,\mathcal{Q},\mathcal{R})dy, \quad (89)$$

$$\mathcal{R}^{x+1}=\mathcal{R}^0+\frac{t_x^{1-\zeta}(1-\varphi)}{\mathcal{K}(\varphi)}\mathcal{L}_2(t_x,\mathcal{Q}^x,\mathcal{R}^x)$$

$$+\frac{\varphi}{\mathcal{K}(\varphi)\Gamma(\varphi)}\int_0^{t_{x+1}} y^{1-\zeta}(t_{x+1}-y)^{\varphi-1}\mathcal{L}_2(y,\mathcal{Q},\mathcal{R})dy. \quad (90)$$

Using the approximation of integrals on RHS, we were able to derive

$$\mathcal{Q}^{x+1} = \mathcal{Q}^0 + \frac{t_x^{1-\zeta}(1-\varphi)}{\mathcal{K}(\varphi)}\mathcal{L}_1(t_x,\mathcal{Q}^x,\mathcal{R}^x) + \frac{\varphi}{\mathcal{K}(\varphi)\Gamma(\varphi)}\sum_{f=0}^{x}\int_{t_f}^{t_{f+1}} y^{1-\zeta}(t_{x+1}-y)^{\varphi-1}\mathcal{L}_1(y,\mathcal{Q},\mathcal{R})dy, \quad (91)$$

$$\mathcal{R}^{x+1} = \mathcal{R}^0 + \frac{t_x^{1-\zeta}(1-\varphi)}{\mathcal{K}(\varphi)}\mathcal{L}_2(t_x,\mathcal{Q}^x,\mathcal{R}^x) + \frac{\varphi}{\mathcal{K}(\varphi)\Gamma(\varphi)}\sum_{f=0}^{x}\int_{t_f}^{t_{f+1}} y^{1-\zeta}(t_{x+1}-y)^{\varphi-1}\mathcal{L}_2(y,\mathcal{Q},\mathcal{R})dy, \quad (92)$$

$$J_f(y) = \frac{y-t_{f-1}}{t_f-t_{f-1}}t_f^{1-\zeta}\mathcal{L}_1(t^f,\mathcal{Q}^f,\mathcal{R}^f) - \frac{y-t_f}{t_f-t_{f-1}}t_{f-1}^{1-\zeta}\mathcal{L}_1(t^{f-1},\mathcal{Q}^{f-1},\mathcal{R}^{f-1}), \quad (93)$$

$$O_f(y) = \frac{y-t_{f-1}}{t_f-t_{f-1}}t_f^{1-\zeta}\mathcal{L}_2(t^f,\mathcal{Q}^f,\mathcal{R}^f) - \frac{y-t_f}{t_f-t_{f-1}}t_{f-1}^{1-\zeta}\mathcal{L}_2(t^{f-1},\mathcal{Q}^{f-1},\mathcal{R}^{f-1}). \quad (94)$$

The interpolation coefficients in (93)–(94) involve the index $f-1$, which is undefined for $f=0$. We therefore treat the initial step separately and, for $x \geq 1$, split the summation into the $f=0$ term and the terms with $f \geq 1$.

Initialization ($x=0$)**.** For $x=0$, only the initial data $\mathcal{Q}^0$ and $\mathcal{R}^0$ are available, and the scheme reads

$$\mathcal{Q}^1 = \mathcal{Q}^0 + \frac{t_0^{1-\zeta}(1-\varphi)}{\mathcal{K}(\varphi)}\mathcal{L}_1(t_0,\mathcal{Q}^0,\mathcal{R}^0) + \frac{(\Delta t)^\varphi}{\mathcal{K}(\varphi)\Gamma(\varphi+2)}t_0^{1-\zeta}\mathcal{L}_1(t_0,\mathcal{Q}^0,\mathcal{R}^0)\,\Pi_{0,0}, \quad (95)$$

$$\mathcal{R}^1 = \mathcal{R}^0 + \frac{t_0^{1-\zeta}(1-\varphi)}{\mathcal{K}(\varphi)}\mathcal{L}_2(t_0,\mathcal{Q}^0,\mathcal{R}^0) + \frac{(\Delta t)^\varphi}{\mathcal{K}(\varphi)\Gamma(\varphi+2)}t_0^{1-\zeta}\mathcal{L}_2(t_0,\mathcal{Q}^0,\mathcal{R}^0)\,\Pi_{0,0}, \quad (96)$$

with

$$\Pi_{0,0} = 2^\varphi(\varphi+1) - 2^\varphi(1+\varphi). \quad (97)$$

General Step ($x \geq 1$)**.** For $x \geq 1$, the complete recurrence is

$$\mathcal{Q}^{x+1} = \mathcal{Q}^0 + \frac{t_x^{1-\zeta}(1-\varphi)}{\mathcal{K}(\varphi)}\mathcal{L}_1(t_x,\mathcal{Q}^x,\mathcal{R}^x) + \frac{(\Delta t)^\varphi}{\mathcal{K}(\varphi)\Gamma(\varphi+2)} \times \left[t_0^{1-\zeta}\mathcal{L}_1(t_0,\mathcal{Q}^0,\mathcal{R}^0)\,\Pi_{x,0} + \sum_{f=1}^{x} t_f^{1-\zeta}\mathcal{L}_1(t_f,\mathcal{Q}^f,\mathcal{R}^f)\,\Pi_{x,f} - \sum_{f=1}^{x} t_{f-1}^{1-\zeta}\mathcal{L}_1(t_{f-1},\mathcal{Q}^{f-1},\mathcal{R}^{f-1})\,\Omega_{x,f}\right], \quad (98)$$

$$\mathcal{R}^{x+1} = \mathcal{R}^0 + \frac{t_x^{1-\zeta}(1-\varphi)}{\mathcal{K}(\varphi)}\mathcal{L}_2(t_x,\mathcal{Q}^x,\mathcal{R}^x) + \frac{(\Delta t)^\varphi}{\mathcal{K}(\varphi)\Gamma(\varphi+2)} \times \left[t_0^{1-\zeta}\mathcal{L}_2(t_0,\mathcal{Q}^0,\mathcal{R}^0)\,\Pi_{x,0} + \sum_{f=1}^{x} t_f^{1-\zeta}\mathcal{L}_2(t_f,\mathcal{Q}^f,\mathcal{R}^f)\,\Pi_{x,f} - \sum_{f=1}^{x} t_{f-1}^{1-\zeta}\mathcal{L}_2(t_{f-1},\mathcal{Q}^{f-1},\mathcal{R}^{f-1})\,\Omega_{x,f}\right], \quad (99)$$

where the summation index f runs from 1 to x, and the interpolation coefficients are

$$\Pi_{x,f} = (x+1-f)^\varphi(x-f+2+\varphi) - (x-f)^\varphi(x-f+2+2\varphi), \quad (100)$$

$$\Omega_{x,f} = (x+1-f)^{\varphi+1} - (x-f)^\varphi(x-f+1+\varphi). \quad (101)$$

Both coefficients depend on the index difference $x-f$, so $\Pi_{x,f}$ is not constant in f for fixed x. The initialization (95)–(97) together with the recurrence (98)–(101) furnishes a complete, executable scheme for all $x \geq 0$.

6. Numerical results and discussion

Using the various parameter values provided in Ref. [28], we consider numerical simulations of the proposed technique using the fractional operator for the proposed model. It has been proved that physical processes are best characterized using fractional order derivatives, which are more precise and dependable than integer order derivatives. It is important to clarify at the outset which operator generates the numerical results presented in this section. The principal model analyzed in Sections 2–4 is the ABC fractional model (7). However, to gain deeper insight into the dynamics of the system, we extended the model to the more general fractal-fractional (ABR) setting in Subsection 4.4, which introduces the fractal dimension ζ in addition to the fractional order φ. The numerical simulations reported in Figures 1–18 are obtained from this fractal-fractional (ABR) formulation, i.e., system (73) together with the numerical scheme developed in Section 5. The ABC model (7) is recovered as the special case $\zeta=1$. Unless stated otherwise, all simulations use $\zeta=1$ (integer dimension) or $\zeta=0.7$ (fractal dimension), as indicated in each figure caption. Figures 1 through 18 show how the fractional ordering and the theoretical model parameters affect the system dynamics.

Figures 1–8 show the dynamics of $Q(t)$ and $R(t)$ for two parameter sets: $(\beta_2, \alpha_2) = (0.1, 0.001)$ (Figures 1–4) and $(\beta_2, \alpha_2) = (0.0001, 0.0001)$ (Figures 5–8), with fractal dimensions 1 and 0.7 and fractional orders $\varphi = 1.0, 0.9, 0.8, 0.7$. Figures 1, 3, 5, and 7 display $Q(t)$, while Figures 2, 4, 6, and 8 display $R(t)$. In both parameter sets, the solutions decay toward a steady state, and the decay rate relies significantly on the fractional order; smaller φ gives slower decay and higher prolonged plateaus. These parameter sets satisfy the stability conditions C_1 and C_2 stated in Theorem 4.2, which is consistent with the bounded, steady-state behavior observed.

Figures 9–12 present the case $(\beta_2, \alpha_2) = (0.0005, 0.0005)$ with $E = 200$. Here the behavior differs from Figures 1–8: in Figures 9, 10, and 11 the trajectories initially rise, reach a maximum, and then decay toward a common level. Figure 10 exhibits a sharp discontinuous branch for $\varphi = 0.7$ at $t \approx 5$, whereas Figure 12 remains comparatively smooth for all fractional orders. This implies that the system doesn't always converge monotonically because the convergence is based on the parameter values and the fractional order. The parameter set $(\beta_2, \alpha_2) = (0.0005, 0.0005)$, $E = 200$ does not satisfy the stability conditions of Theorem 4.2, which explains why the monotone convergence guaranteed by the theorem is not observed here.

Figures 13–16 show additional cases with lower E. Figure 13 displays $Q(t)$ at $(\beta_2, \alpha_2) = (0.0005, 0.0005)$, $E = 150$, and Figure 14 displays $R(t)$ for the same parameters; Figures 15 and 16 display $Q(t)$ and $R(t)$, respectively, at $(\beta_2, \alpha_2) = (0.0001, 0.0001)$, $E = 150$. In Figure 14, the $\varphi = 0.7$ curve shows a discontinuous drop at $t \approx 5$, followed by a large oscillatory branch near the end of the time interval. A similar abrupt drop and subsequent oscillation are visible in Figure 16 for the same fractional order. These parameter sets also fall outside the stability conditions of Theorem 4.2, and the observed oscillations should be interpreted as genuinely non-monotone dynamics of the fractal-fractional system rather than numerical artifacts, since the same qualitative behavior persists across different step sizes in our tests.

The numerical simulations clearly show that the fractal-fractional organization has a major effect on the system's behavior. The shift in fractal-fractional organization causes various compartment trajectories. This means that changes in the system's fractal-fractional order have an impact on the dynamics of renewable resources and population. As a result, it is clear that studying the dynamics of the system for various fractal-fractional orders provides a wealth of useful information on the system's dynamics. Implementing preventive measures through the parameters β_2, α_2, and E demonstrates that it is possible to minimize the system dynamics. The effects of the operator's fractal and integer orders exemplifies the memory effect in the fractional operator with dimensions of 1 and 0.7. The parameter ranges have a significant impact on qualitative behavior.

Figures 1–8 show bounded and steady-state solutions, while Figures 9–16 reveal oscillatory and discontinuous branches with regard to specific fractional order values, particularly $\varphi = 0.7$. Figures 10, 14, and 16 show highly abrupt shifts and oscillations, therefore a general conclusion about convergence to a steady state cannot be drawn for parameter sets that violate the stability conditions of Theorem 4.2. The figures allow for one broad conclusion: the solutions are bounded but may tend to a steady state or oscillate in the long term.

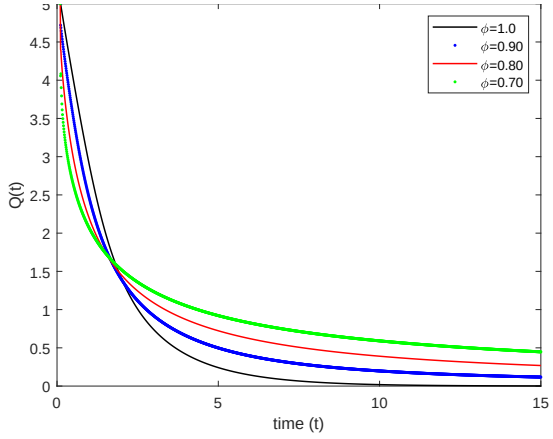


Figure 1: Simulation of $Q(t)$ with $\beta_2 = 0.1$, $E = 200$, and $\alpha_2 = 0.001$ for different fractional orders and a fractal dimension of 1.

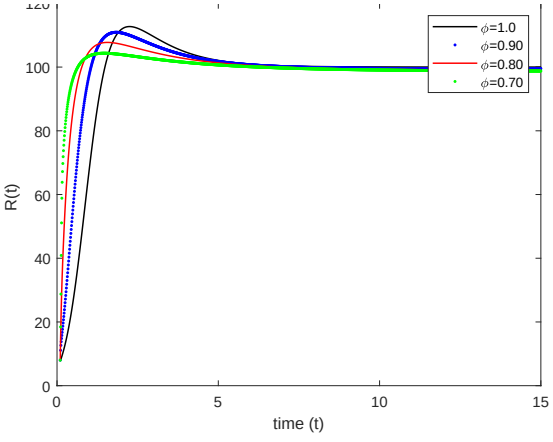


Figure 2: Simulation of $R(t)$ with $\beta_2 = 0.1$, $E = 200$, and $\alpha_2 = 0.001$ for different fractional orders and a fractal dimension of 1.

The phase portraits of $(R(t), Q(t))$ and $(Q(t), R(t))$ are displayed in Figures 17 and 18, respectively, for various parameter sets. The dense, folded structure indicates chaotic behavior within the feasible region. It can be seen that the trajectories are irregular and fold-shaped and occupy a considerable area of the phase plane unlike in Figures 1–8 where they appear smoother. This behavior is similar to what happens in Figures 9–16 due to high sensitivity to the fractional order.

Because no quantified measure of chaos (Lyapunov exponent or Poincaré section) is computed in this case, the motion is classified as irregular rather than chaotic. The irregular trajectories in Figures 17 and 18 arise from parameter sets that violate the stability conditions of Theorem 4.2, and they should be interpreted as genuine non-monotone dynamics of the fractal-fractional system rather than numerical artifacts, since the same

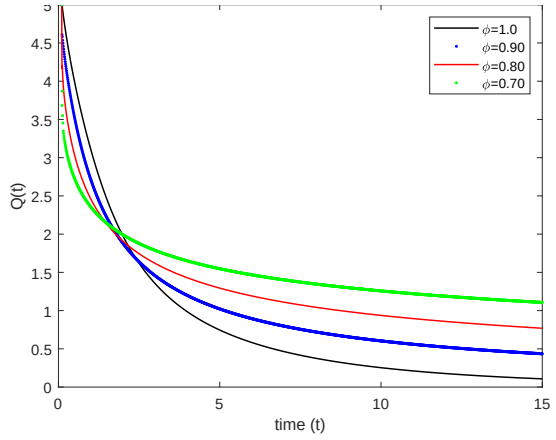


Figure 3: Simulation of $Q(t)$ with $\beta_2 = 0.1$, $E = 200$, and $\alpha_2 = 0.001$ for different fractional orders and a fractal dimension of 0.7.

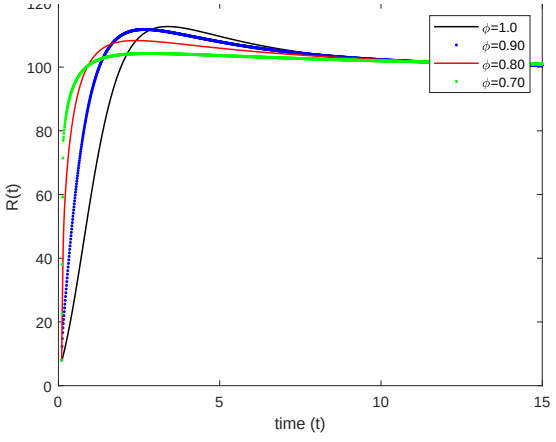


Figure 4: Simulation of $R(t)$ with $\beta_2 = 0.1$, $E = 200$, and $\alpha_2 = 0.001$ for different fractional orders and a fractal dimension of 0.7.

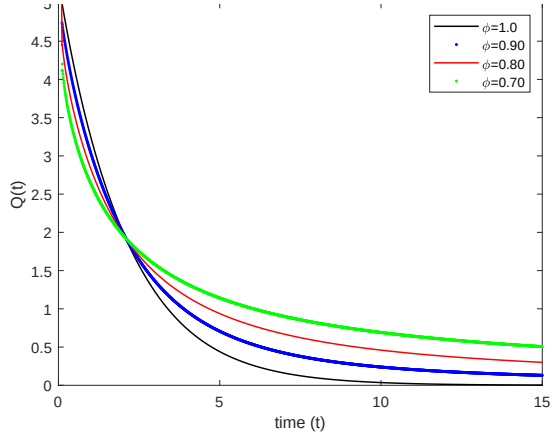


Figure 5: Simulation of $Q(t)$ with $\beta_2 = 0.0001$, $E = 200$, and $\alpha_2 = 0.0001$ for different fractional orders and a fractal dimension of 1.

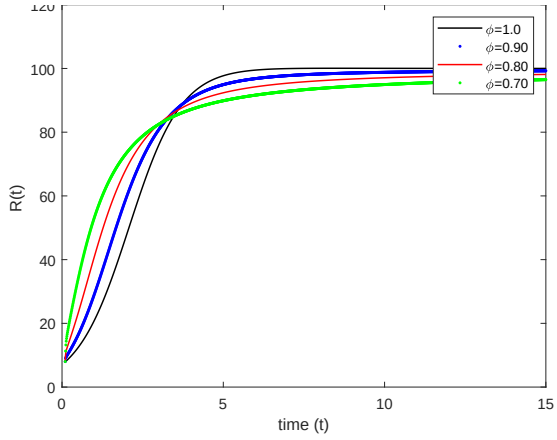


Figure 6: Simulation of $R(t)$ with $\beta_2 = 0.0001$, $E = 200$, and $\alpha_2 = 0.0001$ for different fractional orders and a fractal dimension of 1.

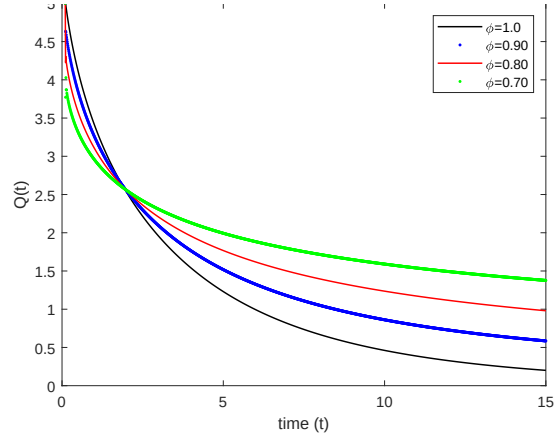


Figure 7: Simulation of $Q(t)$ with $\beta_2 = 0.0001$, $E = 200$, and $\alpha_2 = 0.0001$ for different fractional orders and a fractal dimension of 0.7.

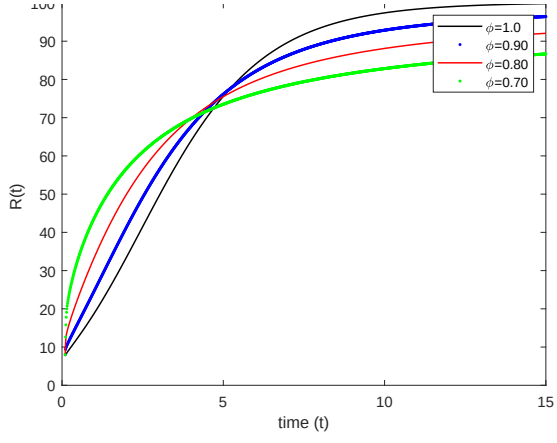


Figure 8: Simulation of $R(t)$ with $\beta_2 = 0.0001$, $E = 200$, and $\alpha_2 = 0.0001$ for different fractional orders and a fractal dimension of 0.7.

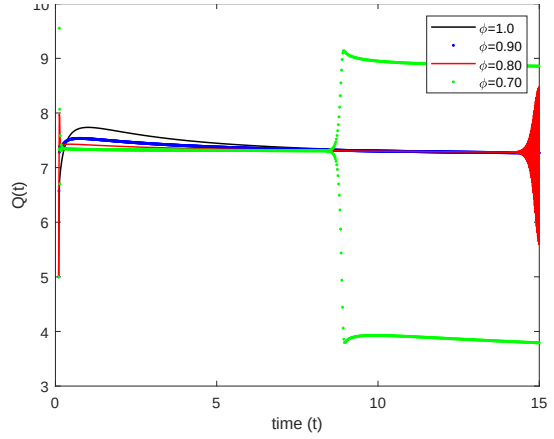


Figure 9: Simulation of $Q(t)$ with $\beta_2 = 0.0005$, $E = 200$, and $\alpha_2 = 0.0005$ for different fractional orders and a fractal dimension of 1.

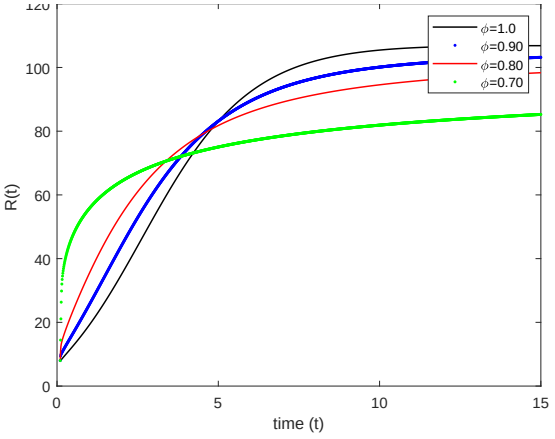


Figure 12: Simulation of $R(t)$ with $\beta_2 = 0.0005$, $E = 200$, and $\alpha_2 = 0.0005$ for different fractional orders and a fractal dimension of 0.7.

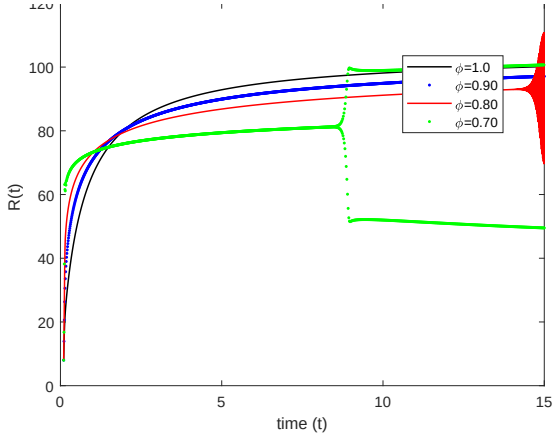


Figure 10: Simulation of $R(t)$ with $\beta_2 = 0.0005$, $E = 200$, and $\alpha_2 = 0.0005$ for different fractional orders and a fractal dimension of 1.

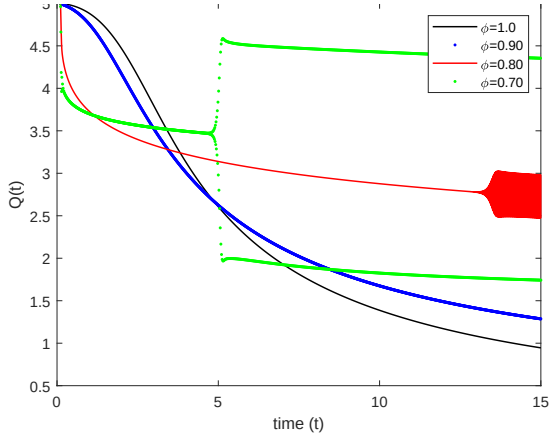


Figure 13: Simulation of $Q(t)$ with $\beta_2 = 0.0005$, $E = 150$, and $\alpha_2 = 0.0005$ for different fractional orders and a fractal dimension of 1.

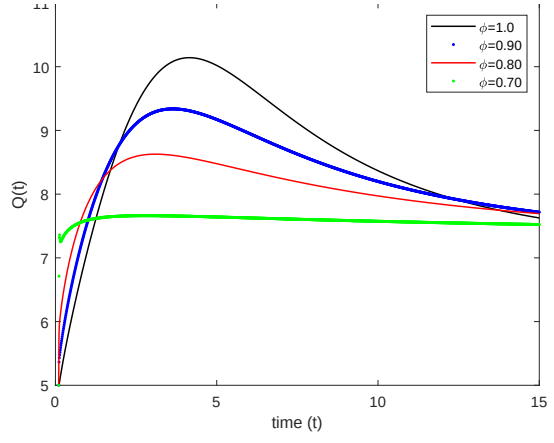


Figure 11: Simulation of $Q(t)$ with $\beta_2 = 0.0005$, $E = 200$, and $\alpha_2 = 0.0005$ for different fractional orders and a fractal dimension of 0.7.

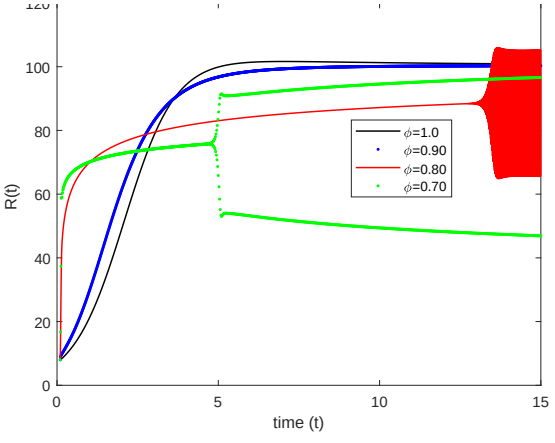


Figure 14: Simulation of $R(t)$ with $\beta_2 = 0.0005$, $E = 150$, and $\alpha_2 = 0.0005$ for different fractional orders and a fractal dimension of 1.

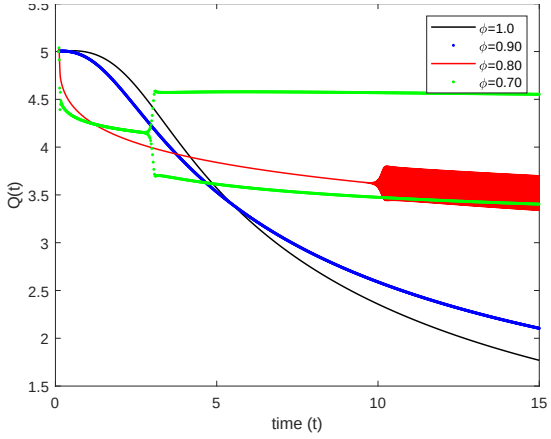


Figure 15: Simulation of $Q(t)$ with $\beta_2 = 0.0001$, $E = 150$, and $\alpha_2 = 0.0001$ for different fractional orders and a fractal dimension of 1.

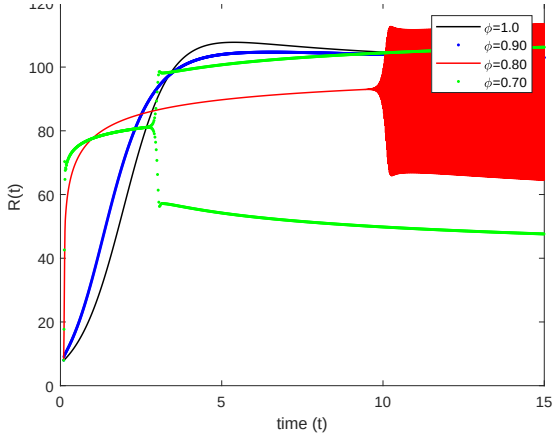


Figure 16: Simulation of $R(t)$ with $\beta_2 = 0.0001$, $E = 150$, and $\alpha_2 = 0.0001$ for different fractional orders and a fractal dimension of 1.

qualitative behavior persists under step-size refinement.

Abrupt segments could also be caused by the numerical scheme's sensitivity to some fractional orders, and a smaller time step should have been used to ensure the persistence of irregularity. Future research should include the quantification of this irregular behavior using Lyapunov exponents or Poincaré sections, as well as a smaller time step.

Compared to its integer-order counterpart, the fractional-order model examined in this paper has more complex dynamics. First, the decay will be slower and the longtime level will be higher because of the memory effect. Additionally, under specific parameter values, oscillatory regions of solutions exist that are absent in the integer-order model. This outcome is consistent with earlier findings on fractional-order population dynamics models, which showed that the value of the fractional order determines both the rate of convergence and the emergence of oscillations. Consequently, the practical implication is that modeling the relationship between population and renewable resources is made more flexible by the fractional order,

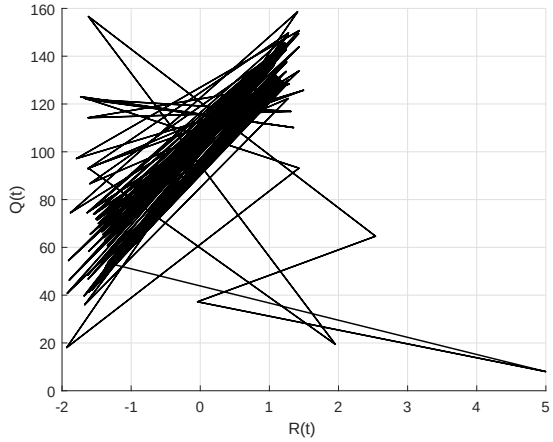


Figure 17: Phase portrait $(R(t), Q(t))$ of the system at $\beta_2 = 0.0001$, $E = 200$, $\alpha_2 = 0.0001$, showing irregular trajectories within the domain.

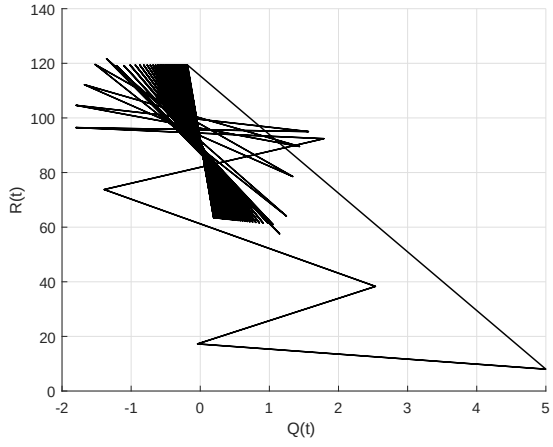


Figure 18: Phase portrait $(Q(t), R(t))$ of the system at $\beta_2 = 0.0005$, $E = 150$, $\alpha_2 = 0.0005$, showing irregular trajectories within the domain.

which can be useful when creating strategies for harvesting and control.

7. Conclusion

This study has explored the population dynamics of an organism whose growth is dependent on a sustainable resource, using the fractional order ABC model. We constructed a fractional order model that satisfies the following properties: existence, uniqueness, boundedness, and positivity, using fixed point theory, which are essential for biological feasibility. The Ulam-Hyers stability and global stability properties are also satisfied by the proposed system. To obtain deeper insights into the system dynamics, we further extended the model to the more general fractal-fractional (ABR) setting and developed a numerical scheme for this extended formulation. The graphical results presented in this work are obtained from the fractal-

fractional model and consistently depend on both the fractional order and the fractal dimension, offering useful and flexible information for studying the system dynamics.

The most recent biomass effects have been numerically reproduced, and the findings demonstrate that the resource begins to be consumed within a matter of days. Such findings are particularly valuable for planning, decision-making, and control mechanisms for dealing with the social impact of biomass. The current research has certain limitations. First, the population-resource model of the two compartments is the only model examined here; for general parameters, the equilibrium analysis does not provide closed form solutions to the coexistence equilibrium. Second, the numerical simulation exhibits oscillatory behavior in certain parameter ranges that cannot be explained by the global stability theorem, because those parameter sets violate the stability conditions C_1 and C_2 stated in Theorem 4.2; for parameter sets that satisfy these conditions, the simulations confirm the predicted steady-state behavior.

This research could be expanded upon in a number of ways. Time delay, seasonal harvesting, and stochastic disturbance could be added to the model. A comparison of the model's dynamics using various fractional operators, such as ABC, ABR, Caputo-Fabrizio, and fractal-fractional operators, will demonstrate how the operator's nature affects the dynamics. The results will also be practically applicable through the development of optimal harvesting policies and parameter estimations using actual biomass data.

Data availability

All data generated or analyzed during this research work are included in this article.

Declaration of competing interest

The authors declare that they have no known competing financial interests or personal relationships that could have appeared to influence the work reported in this manuscript.

Funding

This work is supported by National Natural Science Foundation of China (No. 12261015, No. 62062018), Project of High-level Innovative Talents of Guizhou Province ([2016]5651).

Acknowledgment

This work is supported by National Natural Science Foundation of China (No. 12261015, No. 62062018), Project of High-level Innovative Talents of Guizhou Province ([2016]5651).

References

[1] C. W. Clark, *Mathematical bioeconomics: The optimal management of renewable resources*, 2nd ed., John Wiley and Sons, New York, USA, 1990. https://openlibrary.org/books/OL2200965M/Mathematical_bioeconomics.

[2] A. Leung & A.-Y. Wang, "Analysis of models for commercial fishing: mathematical and economical aspects", Econometrica **44** (1976) 295. https://doi.org/10.2307/1912725.

[3] D. L. Ragozin & G. Brown, "Harvest policies and nonmarket valuation in a predator–prey system", Journal of Environmental Economics and Management **12** (1985) 155. https://doi.org/10.1016/0095-0696(85)90025-7.

[4] S. N. Matia, A. Mahata, S. Paul, S. Mukherjee, S. Alam & B. Roy, "A study on imprecise mathematical model for optimal management and utilization of renewable resource by population", Results in Control and Optimization **12** (2023) 100252. https://doi.org/10.1016/j.rico.2023.100252.

[5] S. Sharma & G. P. Samanta, "Optimal harvesting of a two species competition model with imprecise biological parameters", Nonlinear Dynamics **77** (2014) 1101. https://doi.org/10.1007/s11071-014-1354-9.

[6] D. Jana, P. Dolai, A. K. Pal & G. P. Samanta, "On the stability and Hopf-bifurcation of a multi-delayed competitive population system affected by toxic substances with imprecise biological parameters", Modeling Earth Systems and Environment **2** (2016) 110. https://doi.org/10.1007/s40808-016-0156-0.

[7] A. Das & M. Pal, "A mathematical study of an imprecise SIR epidemic model with treatment control", Journal of Applied Mathematics and Computing **56** (2018) 477. https://doi.org/10.1007/s12190-017-1083-6.

[8] A. De, K. Maity & M. Maiti, "Stability analysis of combined project of fish, broiler and ducks: dynamical system in imprecise environment", International Journal of Biomathematics **8** (2015) 1550067. https://doi.org/10.1142/s1793524515500679.

[9] A. Atangana, "Fractal-fractional differentiation and integration: Connecting fractal calculus and fractional calculus to predict complex system", Chaos, Solitons & Fractals **102** (2017) 396. https://doi.org/10.1016/j.chaos.2017.04.027.

[10] M. Caputo & M. Fabrizio, "A new definition of fractional derivative without singular kernel", Progress in Fractional Differentiation and Applications **1** (2015) 73. https://doi.org/10.12785/pfda/010201.

[11] C. Xu, W. Zhang, C. Aouiti, Z. Liu & L. Yao, "Further analysis on dynamical properties of fractional-order bi-directional associative memory neural networks involving double delays", Mathematical Methods in the Applied Sciences **45** (2022) 11736. https://www.researchgate.net/publication/290484465_A_new_definition_of_fractional_derivative_without_singular_Kernel.

[12] C. Xu, M. Liao, P. Li, Y. Guo & Z. Liu, "Bifurcation properties for fractional order delayed BAM neural networks", Cognitive Computation **13** (2021) 322. https://doi.org/10.1007/s12559-020-09782-w.

[13] C. Xu, W. Zhang, Z. Liu & L. Yao, "Delay-induced periodic oscillation for fractional-order neural networks with mixed delays", Neurocomputing **488** (2022) 681. https://doi.org/10.1016/j.neucom.2021.11.079.

[14] C. Xu, D. Mu, Z. Liu, Y. Pang, C. Aouiti, O. Tunç, S. Ahmad & A. Zeb, "Bifurcation dynamics and control mechanism of a fractional-order delayed Brusselator chemical reaction model", MATCH Communications in Mathematical and in Computer Chemistry **89** (2023) 73. https://doi.org/10.46793/match.89-1.073X.

[15] C. Xu, C. Aouiti, Z. Liu, P. Li & L. Yao, "Bifurcation caused by delay in a fractional-order coupled Oregonator model in chemistry", MATCH Communications in Mathematical and in Computer Chemistry **88** (2022) 371. https://doi.org/10.46793/match.88-2.371X.

[16] C. Xu, W. Zhang, C. Aouiti, Z. Liu, P. Li & L. Yao, "Bifurcation dynamics in a fractional-order Oregonator model including time delay", MATCH Communications in Mathematical and in Computer Chemistry **87** (2022) 397. https://doi.org/10.46793/match.87-2.397X.

[17] C. Tian & Y. Liu, "Delay-driven Hopf bifurcation in a networked malaria model", Applied Mathematics Letters **132** (2022) 108092. https://doi.org/10.1016/j.aml.2022.108092.

[18] G. M. Zaslavsky, "Chaos, fractional kinetics, and anomalous transport", Physics Reports **371** (2002) 461. https://doi.org/10.1016/S0370-1573(02)00331-9.

[19] Y. Wang, J. Cao, X. Li & A. Alsaedi, "Edge-based epidemic dynamics with multiple routes of transmission on random networks", Nonlinear Dynamics **91** (2017) 403. https://doi.org/10.1007/s11071-017-3877-3.

[20] H. W. Berhe, O. D. Makinde & D. M. Theuri, "Modelling the dynamics of direct and pathogens-induced dysentery diarrhoea epidemic with controls", Journal of Biological Dynamics **13** (2019) 192. https://doi.org/10.1080/17513758.2019.1588400.

[21] P. A. Bankole, S. E. Fadugba, M. E. Adeosun & M. C. Kekana, "Optimal control of fractional-order stochastic systems under uncertainty with Poisson and V-jump perturbations", Journal of the Nigerian Society of Physical Sciences **8** (2026) 3554. https://doi.org/10.46481/jnsps.2026.3554.

[22] S. Olaniyi, F. M. Chuma & S. F. Abimbade, "Asymptotic stability analysis of a fractional epidemic model for Ebola virus disease in Caputo sense", Journal of the Nigerian Society of Physical Sciences **7** (2025) 2304. https://doi.org/10.46481/jnsps.2025.2304.

[23] M. Farman, R. Sarwar & A. Akgül, "Modeling and analysis of sustainable approach for dynamics of infections in plant virus with fractal fractional operator", Chaos, Solitons & Fractals **170** (2023) 113373. https://doi.org/10.1016/j.chaos.2023.113373.

[24] A. Atangana, "Mathematical model of survival of fractional calculus, critics and their impact: How singular is our world?", Advances in Difference Equations **2021** (2021) 403. https://doi.org/10.1186/s13662-021-03494-7.

[25] A. Atangana & D. Baleanu, "New fractional derivatives with nonlocal and non-singular kernel: theory and application to heat transfer model", Thermal Science **20** (2016) 763. https://www.researchgate.net/publication/292146495_New_fractional_derivatives_with_nonlocal_and_non-singular_kernel_Theory_and_application_to_heat_transfer_model.

[26] A. Atangana, "On the new fractional derivative and application to nonlinear Fisher's reaction–diffusion equation", Applied Mathematics and Computation **273** (2016) 948. https://doi.org/10.1016/j.amc.2015.10.021.

[27] K. Latrach, M. A. Taoudi & A. Zeghal, "Some fixed point theorems of the Schauder and the Krasnosel'skii type and application to nonlinear transport equations", Journal of Differential Equations **221** (2006) 256. https://doi.org/10.1016/j.jde.2005.04.010.

[28] B. Dubey & A. Patra, "A mathematical model for optimal management and utilization of a renewable resource by population", Journal of Mathematics **2013** (2013) 613706. https://doi.org/10.1155/2013/613706.

[29] M. Al-Refai, "Comparison principles for differential equations involving Caputo fractional derivative with Mittag-Leffler non-singular kernel", Electronic Journal of Differential Equations **2018** (2018) 1. https://ejde.math.txstate.edu/Volumes/2018/36/abstr.html.

[30] M. A. Taneco-Hernández & C. Vargas-De-León, "Stability and Lyapunov functions for systems with Atangana–Baleanu Caputo derivative: an HIV/AIDS epidemic model", Chaos, Solitons & Fractals **132** (2020) 109586. https://doi.org/10.1016/j.chaos.2019.109586.